Partial-wave analysis of $\overline{K}N$ scattering reactions

H. Zhang, J. Tulpan, M. Shrestha, and D. M. Manley
Department of Physics, Kent State University, Kent, Ohio 44242-0001, USA
(Received 24 May 2013; revised manuscript received 18 July 2013; published 13 September 2013)

We investigate the two-body reactions $\overline{K}N \to \overline{K}N$, $\overline{K}N \to \pi\Lambda$, and $\overline{K}N \to \pi\Sigma$ via single-energy partial-wave analyses in the center-of-mass (c.m.) energy range 1480 to 2100 MeV. The partial-wave amplitudes for these reactions thus extracted were constrained by a multichannel energy-dependent model satisfying unitarity of the partial-wave S matrix. We obtain excellent predictions of differential cross sections, polarizations, polarized cross sections, and cross sections for these reactions from a global energy-dependent solution.

DOI: 10.1103/PhysRevC.88.035204 PACS number(s): 14.20.Jn, 13.30.Eg, 13.75.Jz, 11.80.Et

I. INTRODUCTION AND MOTIVATION

Information on hyperon resonances is generally not as extensive as for nucleon resonances. The study of $\overline{K}N \to \overline{K}N$, $\overline{K}N \to \pi\Lambda$, and $\overline{K}N \to \pi\Sigma$ could lead to the better understanding of Λ^*s and Σ^*s.

Most previous partial-wave analyses (PWAs) of $\overline{K}N \to \overline{K}N$, $\overline{K}N \to \pi\Lambda$, and $\overline{K}N \to \pi\Sigma$ [1–6] were based on the assumption that partial-wave amplitudes could be represented by a simple sum of resonant and background terms. Such an assumption violates unitarity of the partial-wave S matrix. In this work, we report on our investigation of the reactions $K^-p \to K^-p$ and $K^-p \to \overline{K}^0n$; $K^-p \to \pi^0\Lambda$; and $K^-p \to \pi^+\Sigma^-$, $K^-p \to \pi^0\Sigma^0$, and $K^-p \to \pi^-\Sigma^+$ via single-energy analyses and a subsequent energy-dependent analysis. All available differential cross section, polarization, polarized cross section, and cross-section data up to a maximum center-of-mass (c.m.) energy of about 2.1 GeV were fitted. In order to ensure that our amplitudes had a relatively smooth variation with energy, we introduced several constraints that will be described in detail below. The determination of resonance parameters from our subsequent energy-dependent analysis is discussed in Ref. [7].

II. FORMALISM AND FITTING PROCEDURES

Here, we summarize the formalism for the single-energy partial-wave analyses. The differential cross section $d\sigma/d\Omega$ and polarization P for unpolarized scattering of spin-0 mesons off spin-$\frac{1}{2}$ nucleons are given by [8]

$$\frac{d\sigma}{d\Omega} = \lambda\!\!\!^{-2}(|f|^2 + |g|^2), \tag{1}$$

$$P\frac{d\sigma}{d\Omega} = 2\lambda\!\!\!^{-2}\,\mathrm{Im}(fg^*), \tag{2}$$

where $\lambda\!\!\!^{-} = \hbar/k$, with k the magnitude of c.m. momentum of the incoming meson. Here, $f = f(W,\theta)$ and $g = g(W,\theta)$ are the usual spin-nonflip and spin-flip amplitudes at c.m. energy W and meson c.m. scattering angle θ. In terms of partial waves, f and g can be expanded as

$$f(W,\theta) = \sum_{l=0}^{\infty}[(l+1)T_{l+} + lT_{l-}]P_l(\cos\theta), \tag{3}$$

$$g(W,\theta) = \sum_{l=1}^{\infty}[T_{l+} - T_{l-}]P_l^1(\cos\theta), \tag{4}$$

where l is the initial orbital angular momentum, $P_l(\cos\theta)$ is a Legendre polynomial, and $P_l^1(\cos\theta) = \sin\theta \times dP_l(\cos\theta)/d(\cos\theta)$. The total angular momentum for the amplitude T_{l+} is $J = l + \frac{1}{2}$, while that for the amplitude T_{l-} is $J = l - \frac{1}{2}$. For the initial $\overline{K}N$ system, we have $I = 0$ or $I = 1$ so that the amplitudes $T_{l\pm}$ can be expanded in terms of isospin amplitudes as

$$T_{l\pm} = C_0T_{l\pm}^0 + C_1T_{l\pm}^1, \tag{5}$$

where $T_{l\pm}^I$ are partial-wave amplitudes with isospin I and total angular momentum $J = l \pm \frac{1}{2}$, with C_I the appropriate isospin Clebsch-Gordon coefficients for a given reaction. For $K^-p \to K^-p$, for example, we have $C_0 = \frac{1}{2}$ and $C_1 = \frac{1}{2}$.

The total K^-p cross section is given by $\sigma_{\mathrm{total}} = 4\pi\lambda\!\!\!^{-2}\mathrm{Im}\,f(W,0)$, or

$$\sigma_{\mathrm{total}} = 4\pi\lambda\!\!\!^{-2}\sum_{l=0}^{\infty}[(l+1)\,\mathrm{Im}\,T_{l^+} + l\,\mathrm{Im}\,T_{l^-}], \tag{6}$$

where here the $T_{l\pm}$ are partial-wave amplitudes for elastic $\overline{K}N$ scattering.

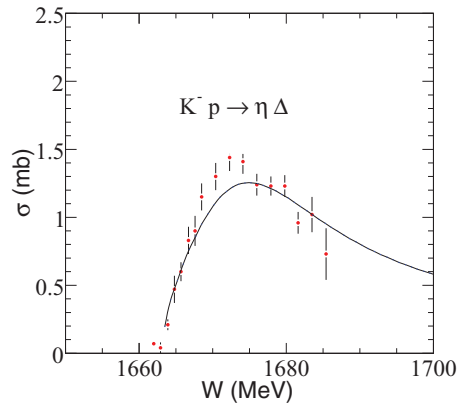

FIG. 1. (Color online) Integrated cross section for $K^-p \to \eta\Lambda$ compared with the results of our energy-dependent fit. Data are from Starostin (2001) [28].

TABLE I. Summary of database for $\overline{K}N \to \overline{K}N$. Column 1 lists the central energy W_0 of each energy bin, columns 2 and 3 list the number of differential cross-section data points in each bin for $K^-p \to K^-p$ and $K^-p \to \overline{K}^0n$, respectively, column 4 lists the number of polarization data points for $K^-p \to K^-p$ in each bin, column 5 lists the number of polarized cross-section data points for $K^-p \to K^-p$ in each bin, column 6 lists the number of integrated cross-section data points for $K^-p \to K^-p$ and $K^-p \to \overline{K}^0n$ in each bin, column 7 lists the number of K^-p total cross-section data points in each bin, column 8 lists the total number of data points for all kinds of data in each bin, and column 9 lists the references for the measurements referred to in columns 2–5.

W_0 (MeV)	$d\sigma/d\Omega$ (K^-p)	$d\sigma/d\Omega$ $(\overline{K}^0n)$	P (K^-p)	$Pd\sigma/d\Omega$ (K^-p)	σ	σ_{total}	Total No.	References
1480	57	24			15	5	96	[9]
1500	114	120			23	8	257	[9]
1520	100	100			28	10	228	[9]
1540	178	120			25	8	323	[9,10]
1560	117	100			14	5	231	[10–12]
1580	78	112			10	3	200	[10–12]
1600	79	116			14	6	209	[10–12]
1620	147	120			14	6	281	[10–13]
1640	113	148			14	6	275	[10–13]
1660	149	132			19	6	300	[10–13]
1680	194	210			30	9	434	[2,10–14]
1700	150	112			11	6	283	[2,10,11,13,14]
1720	150	150			20	6	320	[2,11,13,14]
1740	216	241		27	29	6	513	[2,11,13–16]
1760	176	193		26	25	4	420	[2,11,13–16]
1780	185	196		27	34	9	442	[2,11,14,16–18]
1800	132	79		52	18	4	281	[2,14,16,18]
1820	146	60		27	18	5	251	[2,14,15,18]
1840	185	80		27	23	9	315	[2,14,17,18]
1860	227	100		30	22	4	379	[2,14,17–19]
1880	266	120		28	21	6	435	[2,14,15,18,19]
1900	175	60		56	18	6	309	[2,14,15,17–19]
1920	146	60		27	17	3	250	[17–19]
1940	110	80		30	18	5	238	[15,18,19]
1960	64	40	23		14	4	141	[18–20]
1980	34	20			11	3	65	[19,21]
2000	23	20	23		9	3	75	[20,21]
2020	23		23		12	5	58	[20]
2040	54		22		10	4	86	[20,21]
2060	23		23		10	3	56	[20]
2080	22		22		9	3	53	[20]
2100	53		22		7	2	83	[20,21]
2120	46		23	46	12	5	104	[17,20]
2140	23		23		5	2	51	[20]
2160	32				14	5	46	[21]

The integrated cross section for a particular two-body reaction is

$$\sigma = 4\pi\lambda^2 \sum_{l=0}^{\infty} [(l+1)|T_{l^+}|^2 + l|T_{l^-}|^2]. \tag{7}$$

Tables I, II, and III summarize the available quantity and types of data in each energy bin for the three reactions $\overline{K}N \to \overline{K}N$, $\overline{K}N \to \pi\Lambda$, and $\overline{K}N \to \pi\Sigma$, respectively. Single-energy fits were performed separately for (i) $K^-p \to K^-p$ and $K^-p \to \overline{K}^0n$, for (ii) $K^-p \to \pi^0\Lambda$, and for (iii) $K^-p \to \pi^+\Sigma^-$, $K^-p \to \pi^0\Sigma^0$, and $K^-p \to \pi^-\Sigma^+$. In each case the available data were analyzed in c.m. energy bins of width 20 MeV. This choice of bin width was appropriate because the data for smaller widths had unacceptably low statistics,

TABLE II. Summary of database for $\overline{K}N \to \pi\Lambda$. Column 1 lists the central energy W_0 of each energy bin, column 2 lists the number of differential cross-section data points in each bin for $K^- p \to \pi^0\Lambda$, column 3 lists the number of polarization data points in each bin, column 4 lists the number of polarized cross-section data points in each bin, column 5 lists the number of integrated cross-section data points in each bin, column 6 lists the total number of data points for all kinds of data in each bin, and column 7 lists the references for the measurements referred to in columns 2–4.

W_0 (MeV)	$d\sigma/d\Omega$	P	$Pd\sigma/d\Omega$	σ	Total No.	References
1480				4	4	[22]
1500				8	8	[22]
1520				9	9	[22]
1540	40		16	7	63	[10]
1560	76	16	26	4	122	[10,12]
1580	56	16	19	2	93	[10,12]
1600	56	16	20	5	97	[10,12]
1620	56	16	20	4	96	[10,12]
1640	81	32	20	6	139	[10,12,23]
1660	74	16	19	9	118	[10,12,23]
1680	114	22	28	13	177	[10,12,14,23]
1700	58	7	8	13	86	[10,14,23]
1720	101	27		9	137	[14,16,23]
1740	185	65		12	262	[14,16,23]
1760	138	54		11	203	[14,16,23]
1780	160	88		10	258	[14,16,18]
1800	80	46		4	130	[14,16,18]
1820	60	35		4	99	[14,18]
1840	80	36		5	121	[14,18]
1860	100	26		7	133	[14,18,19]
1880	120	44		7	171	[14,18,19]
1900	60	18		5	83	[14,18,19]
1920	80	21		7	108	[18,19,24]
1940	100	23		8	131	[18,19,24]
1960	60	24		5	89	[18,19,24]
1980	40	6		5	51	[19,24]
2000	40	13		4	57	[19,24]
2020	20	9		4	33	[24]
2040	20	8		2	30	[24]
2060	30	6		3	39	[24,25]
2080	40	8		3	51	[24,25]
2100	30			2	32	[25]
2120	70	11		4	85	[24,25]
2140					0	
2160	40	9		2	51	[24]

and for larger widths some amplitudes varied too much over the energy spread of the bin.

The general qualitative behavior of the partial-wave amplitudes that we wanted to determine is known from earlier partial-wave analyses. Therefore it was convenient to make use of this information in our single-energy fits. In 2007, one of us (J. Tulpan) completed a multichannel fit [27] of published partial-wave amplitudes for $\overline{K}N$ scattering to several final states, including $\overline{K}N, \overline{K}^*N, \overline{K}\Delta, \pi\Lambda, \pi\Lambda(1520)$, $\pi\Sigma$, and $\pi\Sigma(1385)$. The channels $\sigma\Lambda$, $\sigma\Sigma$, and $\eta\Sigma$ (for S_{11}) were included as "dummy channels," where σ denotes the broad isoscalar S-wave $\pi\pi$ interaction. Also, $\eta\Lambda$ was included for S_{01}. Our fit of S_{01} amplitudes included data for $\sigma(K^- p \to \eta\Lambda)$ up to a c.m. energy of 1685 MeV (see Fig. 1). The dummy channels were channels without data and were included to satisfy unitarity in some partial waves. Tulpan's work resulted in an energy-dependent solution that is consistent with S-matrix unitarity. We refer to his solution as the *initial global fit*. Within each energy bin, each partial-wave amplitude with a given isospin

TABLE III. Summary of database for $\overline{K}N \to \pi\Sigma$. Column 1 lists the central energy W_0 of each energy bin; columns 2, 3, and 4 list the number of differential cross-section data points in each bin for $K^-p \to \pi^+\Sigma^-$, $K^-p \to \pi^0\Sigma^0$, and $K^-p \to \pi^-\Sigma^+$, respectively; columns 5 and 6 list the number of polarization data points for $K^-p \to \pi^0\Sigma^0$ and $K^-p \to \pi^-\Sigma^+$, respectively, in each bin; columns 7 and 8 list the number of polarized cross-section data points for $K^-p \to \pi^0\Sigma^0$ and $K^-p \to \pi^-\Sigma^+$, respectively, in each bin; column 9 lists the number of integrated cross-section data points for $K^-p \to \pi^+\Sigma^-$, $K^-p \to \pi^0\Sigma^0$, and $K^-p \to \pi^-\Sigma^+$ in each bin; column 10 lists the total number of data points for all kinds of data in each bin; and column 11 lists the references for the measurements referred to in columns 2–8.

W_0 (MeV)	$d\sigma/d\Omega$ $(\pi^+\Sigma^-)$	$d\sigma/d\Omega$ $(\pi^0\Sigma^0)$	$d\sigma/d\Omega$ $(\pi^-\Sigma^+)$	P $(\pi^0\Sigma^0)$	P $(\pi^-\Sigma^+)$	$Pd\sigma/d\Omega$ $(\pi^0\Sigma^0)$	$Pd\sigma/d\Omega$ $(\pi^-\Sigma^+)$	σ	Total No.	References
1480								13	13	[22]
1500								21	21	[22]
1520								23	23	[22]
1540	40	19	40			19	18	22	158	[10]
1560	60	39	60	9		30	30	12	240	[10,12,26]
1580	40	29	40	9		20	20	6	164	[10,12,26]
1600	40	29	40	9		20	20	10	168	[10,12,26]
1620	40	29	40	9		20	20	13	171	[10,12,26]
1640	40	48	40	18		20	20	11		[10,12,23,26]
1660	40	49	40	9		20	19	17	194	[10,12,23,26]
1680	80	49	80	9		30	29	25	302	[10,12,14,23,26]
1700	40	30	40			10	9	16	145	[10,14,23]
1720	76	30	75		10			15	206	[14,16,23]
1740	154	20	157		24			24	379	[14,16,23]
1760	114	20	114		25			20	293	[14,16,23]
1780	148		147		34			24	353	[14,16,18]
1800	72		74		22			10	178	[14,16,18]
1820	60		60		15			11	146	[14,18]
1840	80		80		13			14	187	[14,18]
1860	100		100		11			18	229	[14,18,19]
1880	120		120		24			18	282	[14,18,19]
1900	60		60		14			8	142	[14,18,19]
1920	80		79		15			12	186	[18,19,24]
1940	99		100		14			17	230	[18,19,24]
1960	60		59		17			10	146	[18,19,24]
1980	40		38					7	85	[19,24]
2000	40		40					9	89	[19,24]
2020	19		19					5	43	[24]
2040	20		16					2	38	[24]
2060	19	10	18					5	52	[24,25]
2080	20	10	19					5	54	[24,25]
2100		26						3	29	[25]
2120	39	8	37					4	88	[24,25]
2140									0	
2160	36		35					5	76	[24]

amplitude was approximated by a first-order Taylor series expansion:

$$T(W) = T(W_0) + T'(W_0)(W - W_0), \tag{8}$$

where W is the c.m. energy of the data point in the bin and W_0 is the central energy of the bin. Here, for simplicity $T(W)$ denotes an isospin amplitude $T^I_{l\pm}$. The complex T-matrix amplitude $T(W_0)$ belongs to the parameter set to be optimized at c.m. energy W_0, and $T'(W_0)$ is called the slope parameter. During fits, the slope parameter was held fixed so that the real and imaginary parts of $T(W_0)$ were our fitting parameters. During our initial single-energy partial-wave analyses, we calculated the slope parameters $T'(W_0)$ from the initial global fit and kept these parameters constant in our fits.

Because the database is somewhat sparse, additional constraints were introduced in order to determine partial-wave amplitudes with a reasonably smooth variation with energy.

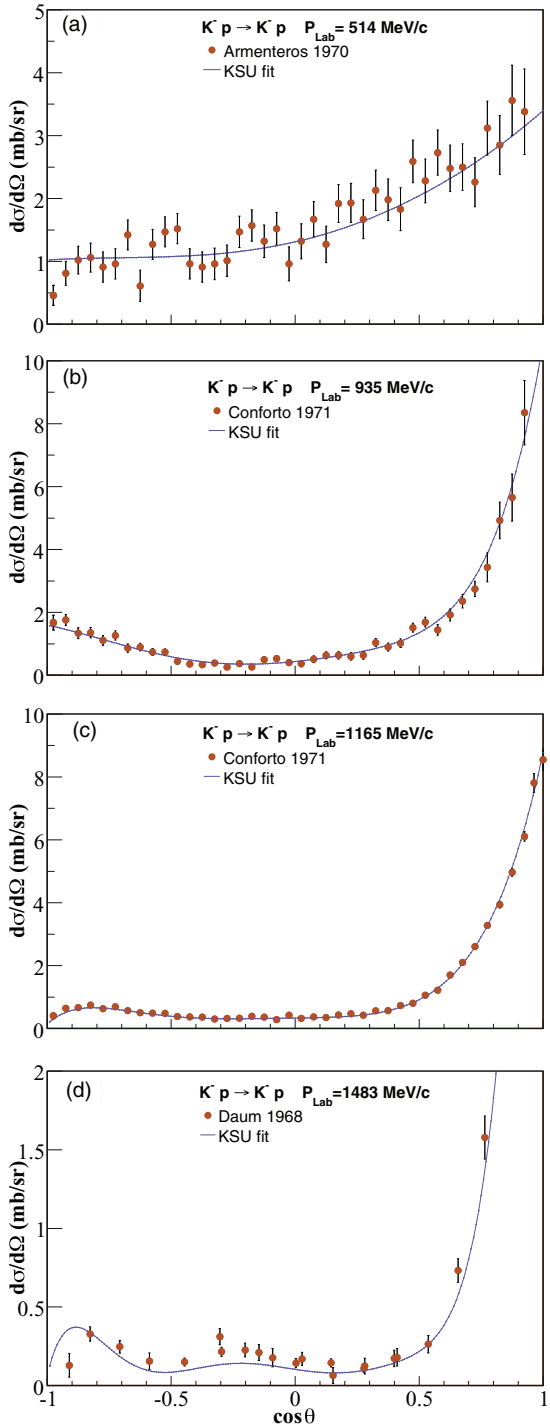

FIG. 2. (Color online) Representative results of our energy-dependent fit for the $K^- p \to K^- p$ differential cross section. Data are from Armenteros (1970) [10], Conforto (1971) [2], and Daum (1968) [20].

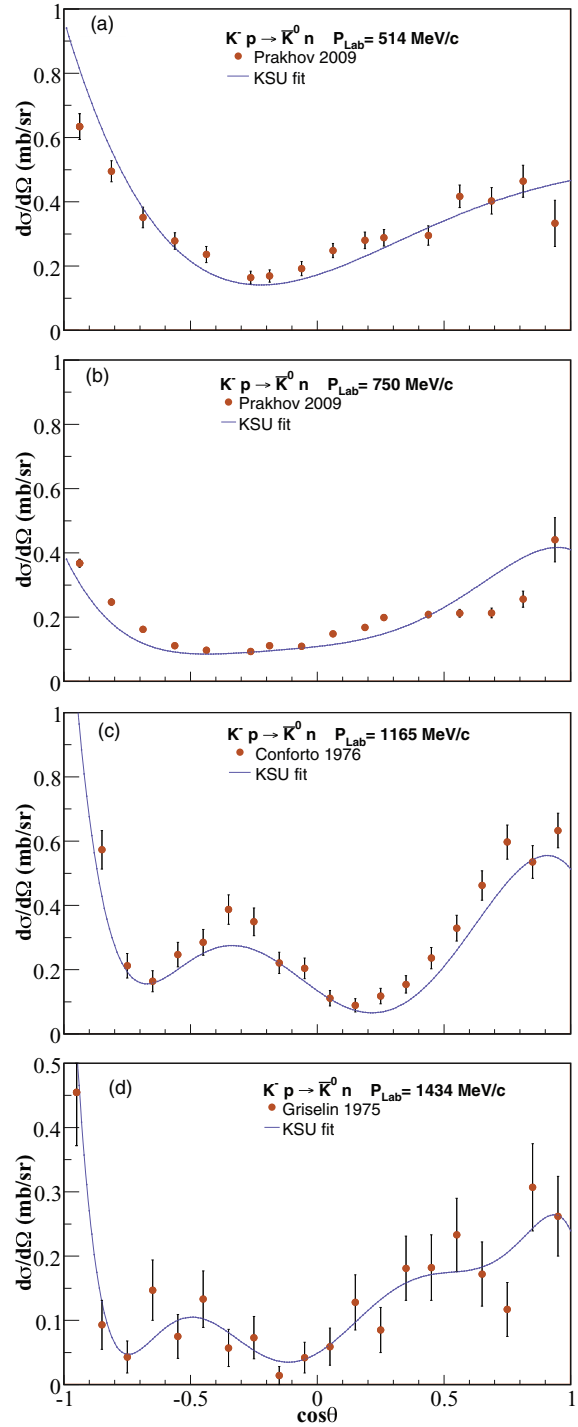

FIG. 3. (Color online) Representative results of our energy-dependent fit for the $K^- p \to \overline{K}^0 n$ differential cross section. Data are from Prakhov (2009) [12], Conforto (1976) [18], and Griselin (1975) [19].

To decrease the number of free parameters to be searched, we also held fixed the very small T-matrix amplitudes (those with $|T(W_0)| < 0.05$). This constraint is expected to introduce only a small bias to our final energy-dependent partial-wave solution.

As an additional constraint, we held fixed the D_{03} amplitudes for $\overline{K}N \to \overline{K}N$ and $\overline{K}N \to \pi\Sigma$ at the values from the initial global fit in the bin with $W_0 = 1520$ MeV. This constraint was introduced because of the well known narrow $\Lambda(1520)$ resonance, which has a width of only about 16 MeV.

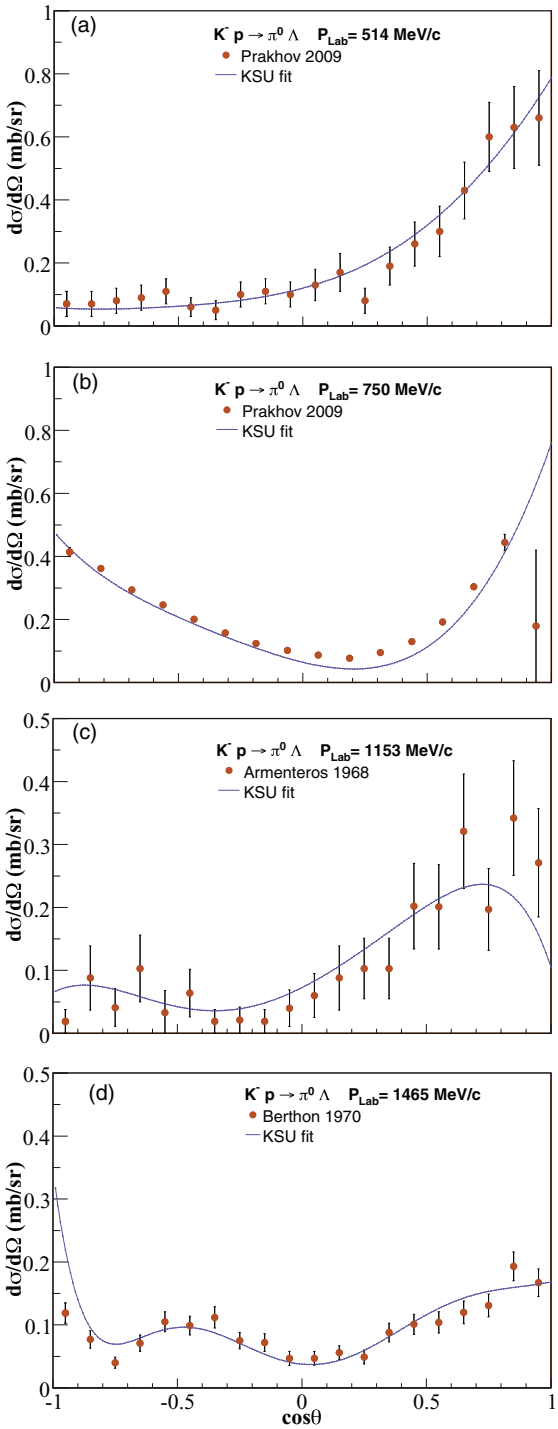

FIG. 4. (Color online) Representative results of our energy-dependent fit for the $K^- p \to \pi^0 \Lambda$ differential cross section. Data are from Prakhov (2009) [12], Armenteros (1968) [14], and Berthon (1970) [24].

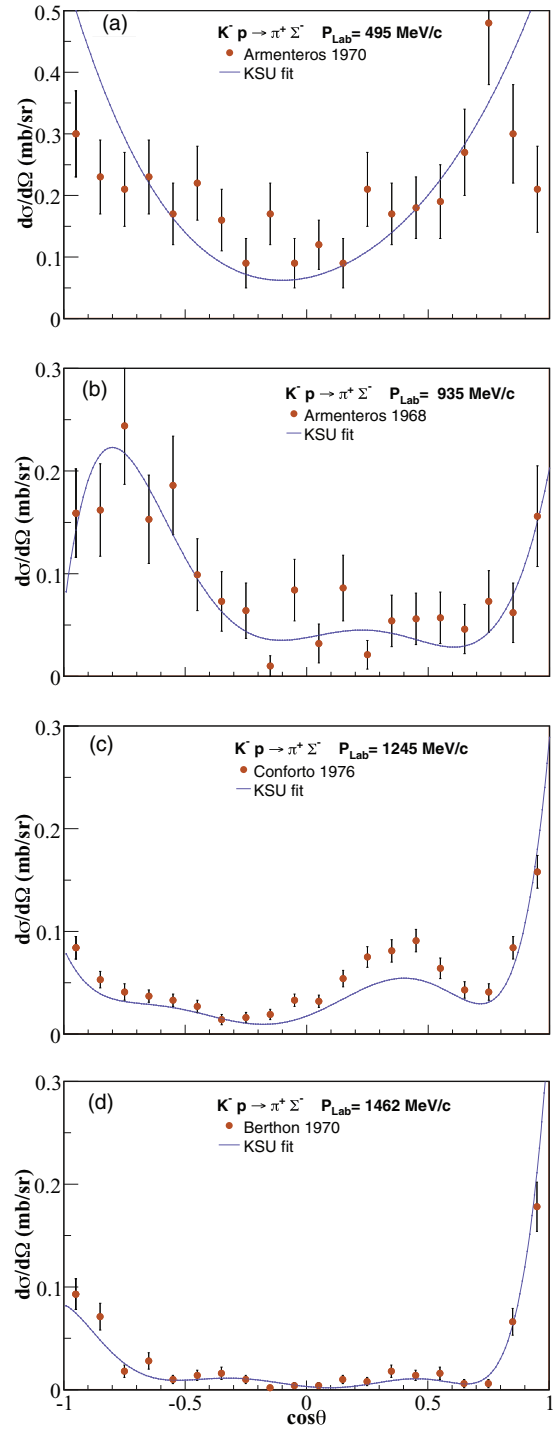

FIG. 5. (Color online) Representative results of our energy-dependent fit for the $K^- p \to \pi^+ \Sigma^-$ differential cross section. Data are from Armenteros (1970) [10], Armenteros (1968) [14], Conforto (1976) [18], and Berthon (1970) [24].

Even with this constraint, we ultimately concluded that we could not determine reliable amplitudes in this bin for the reactions $\overline{K}N \to \overline{K}N$ and $\overline{K}N \to \pi\Sigma$.

Finally, in our single-energy fits, we introduced a *penalty term* to the χ^2 function that we minimized. This penalty term constrained our fitted amplitudes from differing greatly from the values of the initial global fit. For calculating the uncertainties in our single-energy amplitudes, we carried out a *zero-iteration* fit in which the initial values of all amplitudes were replaced by the values determined by our χ^2

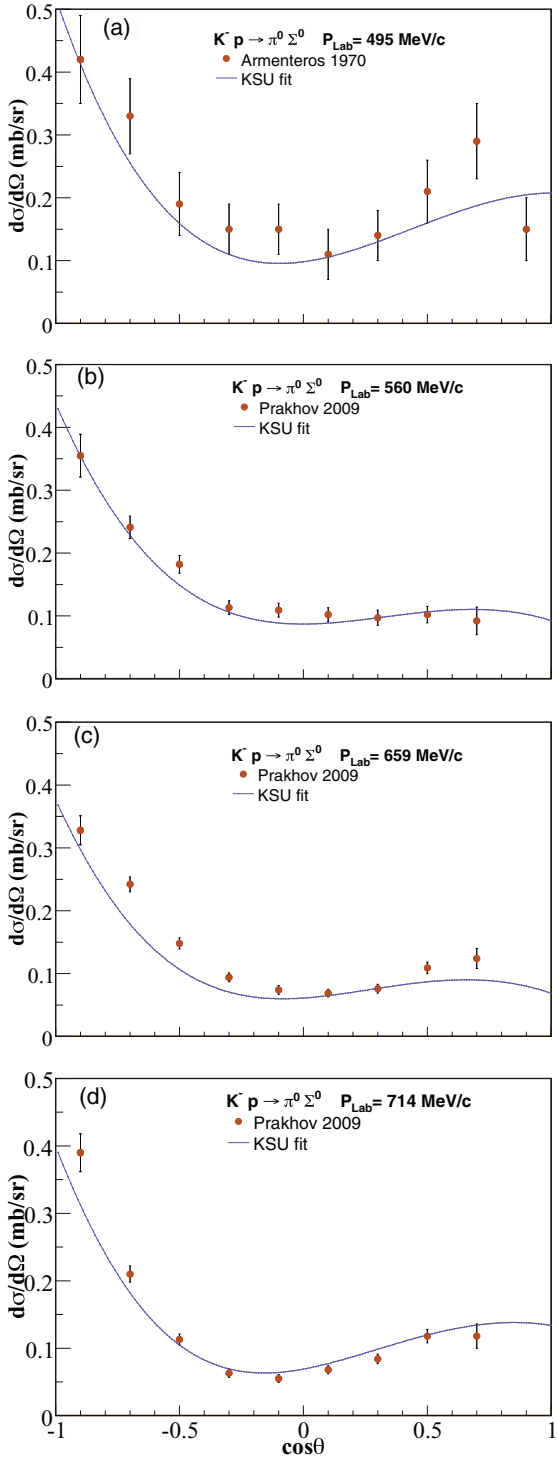

FIG. 6. (Color online) Representative results of our energy-dependent fit for the $K^- p \to \pi^0 \Sigma^0$ differential cross section. Data are from Armenteros (1970) [10] and Prakhov (2009) [12].

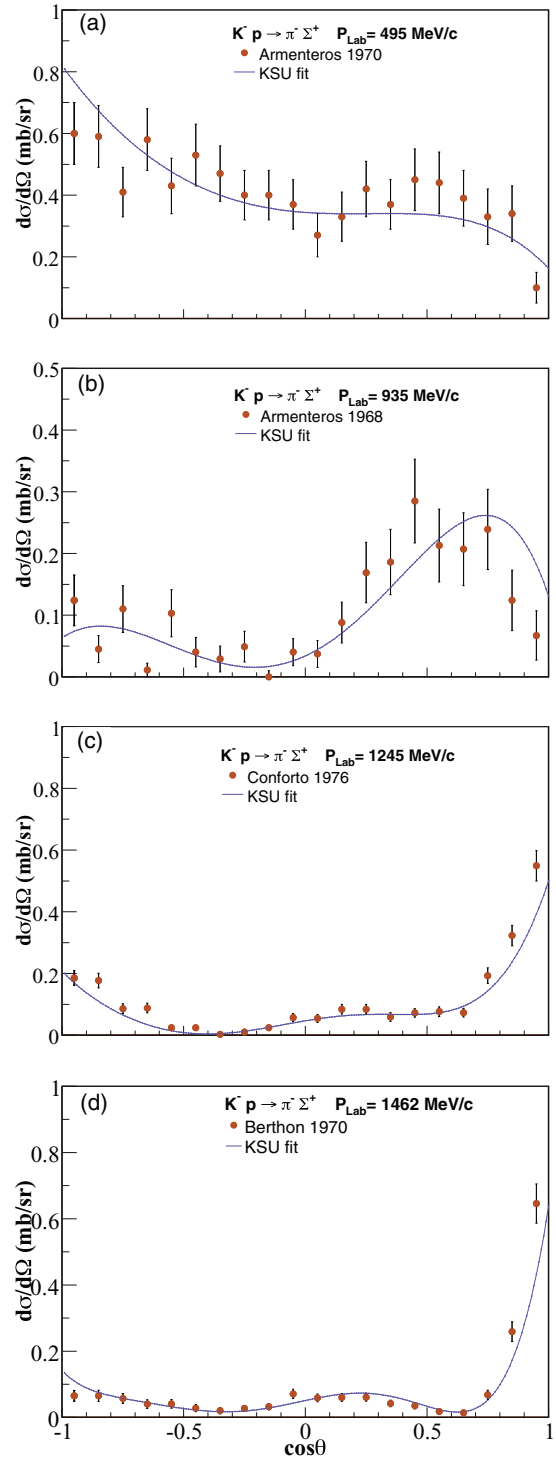

FIG. 7. (Color online) Representative results of our energy-dependent fit for the $K^- p \to \pi^- \Sigma^+$ differential cross section. Data are from Armenteros (1970) [10], Armenteros (1968) [14], Conforto (1976) [18], and Berthon (1970) [24].

minimization procedure. In the zero-iteration fit, all partial-wave amplitudes except G_{17} were treated as free parameters. The G_{17} amplitude was held fixed in this procedure to remove the ambiguity in determining the global overall phase of our amplitudes. Spin-9/2 waves were not needed in our solution.

Once we had obtained a complete set of amplitudes for $\overline{K}N$, $\pi\Lambda$, and $\pi\Sigma$ reactions from our single-energy analyses, we carried out global multichannel energy-dependent fits using a procedure similar to that of Tulpan [27]. The key new

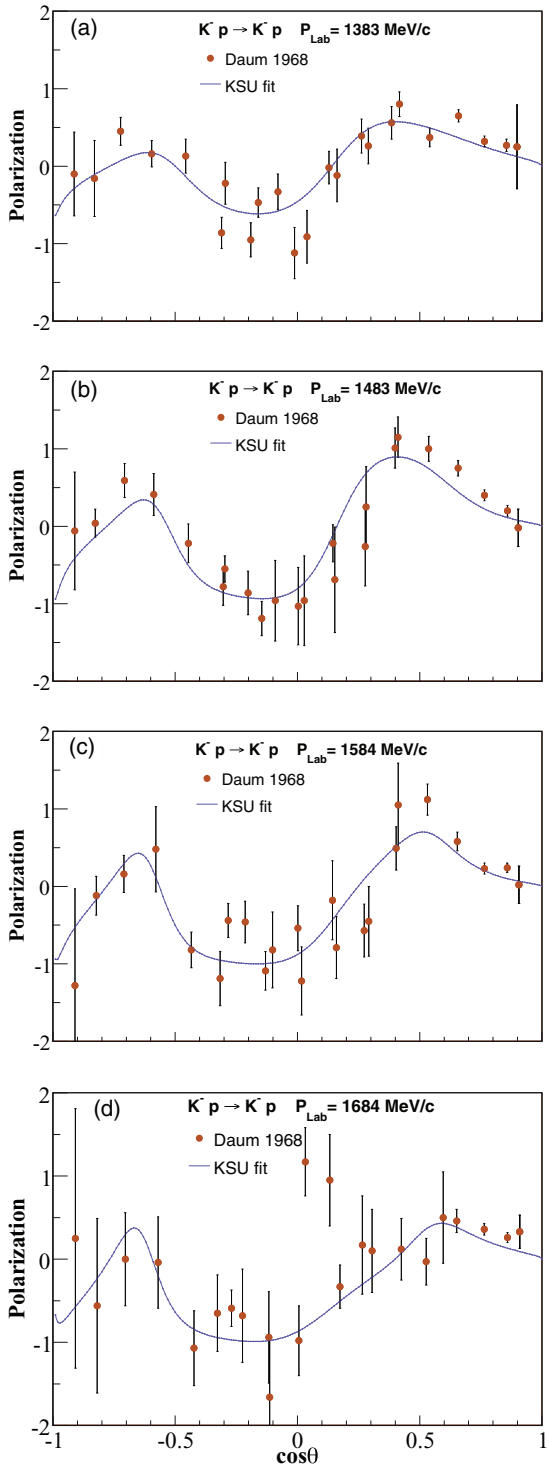

FIG. 8. (Color online) Representative results of our energy-dependent fit for the $K^- p \to K^- p$ polarization. Data are from Daum (1968) [20].

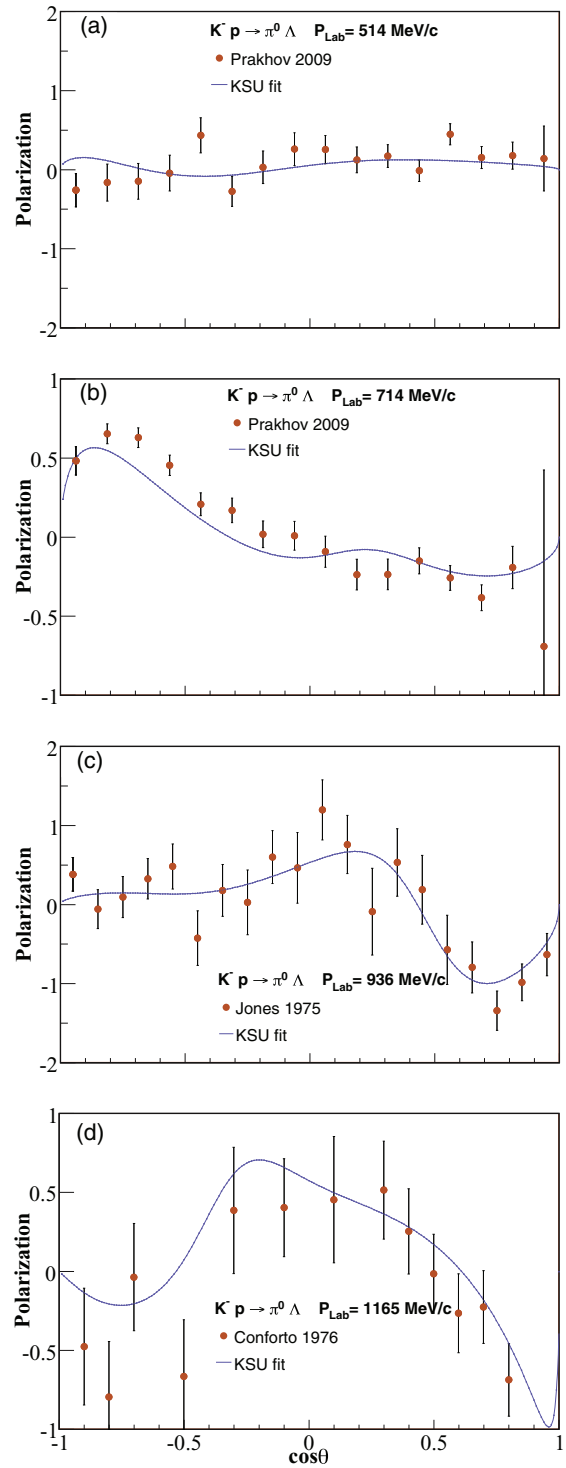

FIG. 9. (Color online) Representative results of our energy-dependent fit for the $K^- p \to \pi^0 \Lambda$ polarization. Data are from Prakhov (2009) [12], Jones (1975) [16], and Conforto (1976) [18].

ingredient is that our global fit (details of how the partial-wave S matrix was constructed can be found in Ref. [29]) used our own single-energy amplitudes for the $\overline{K}N$, $\pi\Lambda$, and $\pi\Sigma$ channels. For other final states, we used the same input information as Tulpan did from Refs. [6,30–33]. We assumed the same uncertainties used by Tulpan [27] for obtaining the inital global fit (± 0.025 for $\overline{K}N$, ± 0.035 for $\pi\Lambda$ and $\pi\Sigma$, and ± 0.050 otherwise). These uncertainties were necessary

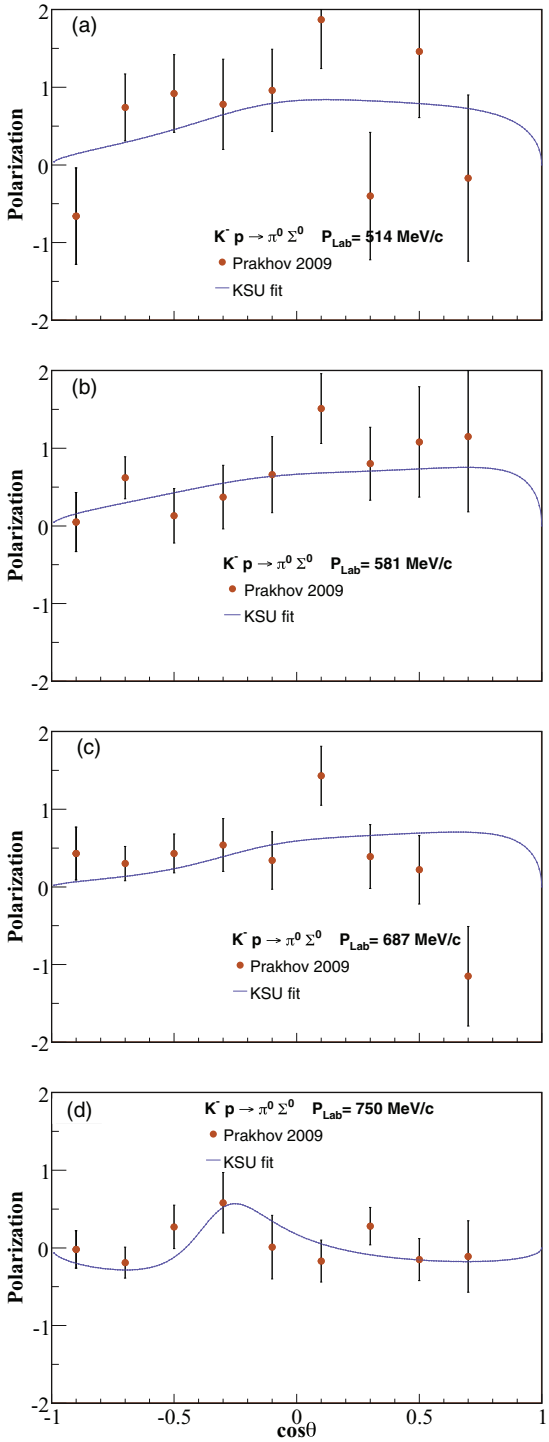

FIG. 10. (Color online) Representative results of our energy-dependent fit for the $K^- p \to \pi^0 \Sigma^0$ polarization. Data are from Prakhov (2009) [12].

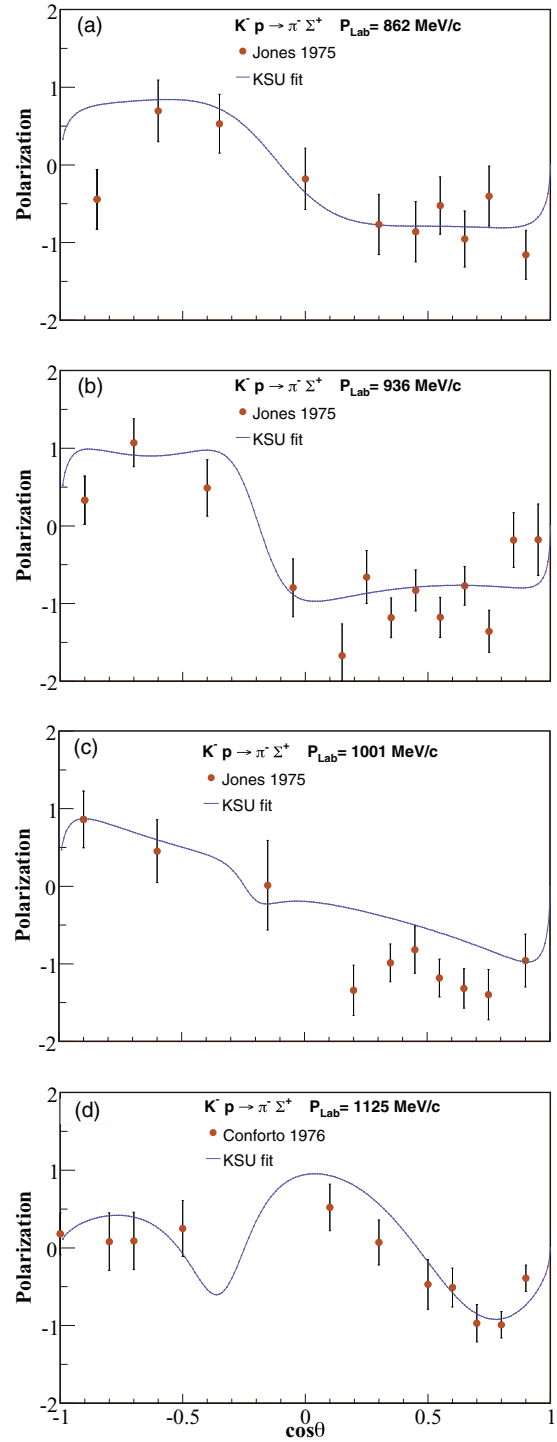

FIG. 11. (Color online) Representative results of our energy-dependent fit for the $K^- p \to \pi^- \Sigma^+$ polarization. Data are from Jones (1975) [16] and Conforto (1976) [18].

because previous published partial-wave amplitudes were without error bars. These uncertainties were estimated by comparing like partial-wave amplitudes from different energy-dependent analyses and estimating the average differences for the real and imaginary parts. The smaller error bars implied the analyses agreed well with each other and the larger error bars implied the analyses agreed less well with each other.

We reduced the number of free amplitudes for a new set of single-energy solutions. At this stage, our free amplitudes included only S_{01}, S_{11}, P_{01}, P_{11}, P_{13}, and D_{03}. All other

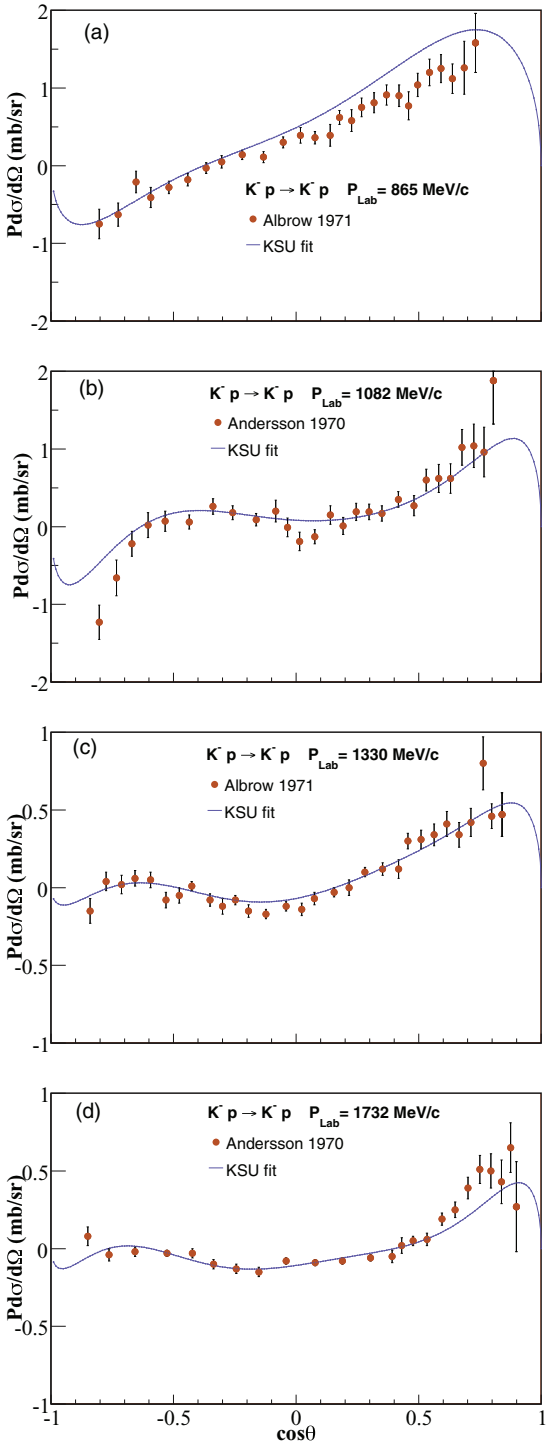

FIG. 12. (Color online) Representative results of our energy-dependent fit for the $K^- p \to K^- p$ polarized cross section. Data are from Albrow (1971) [15] and Andersson (1970) [17].

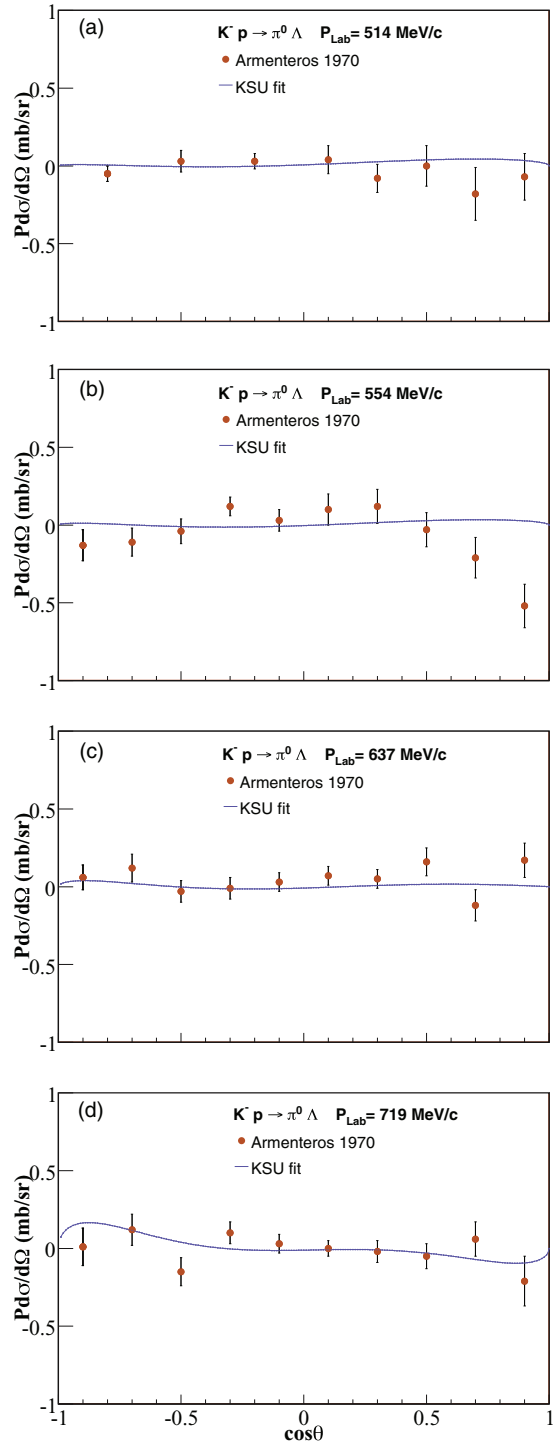

FIG. 13. (Color online) Representative results of our energy-dependent fit for the $K^- p \to \pi^0 \Lambda$ polarized cross section. Data are from Armenteros (1970) [10].

amplitudes were held fixed at the values determined from our first new global fit. In addition, the slope parameters were recalculated based on the new global fit and kept constant during this stage of the single-energy analyses. We were able to obtain excellent agreement with the observables. Next, we repeated our global energy-dependent analysis to refit the new set of single-energy amplitudes for S_{01}, S_{11}, P_{01}, P_{11}, P_{13}, and D_{03}. We then compared our new predictions with the observables in our single-energy fits. Still the agreement was less than satisfactory, so we carried out yet another round of

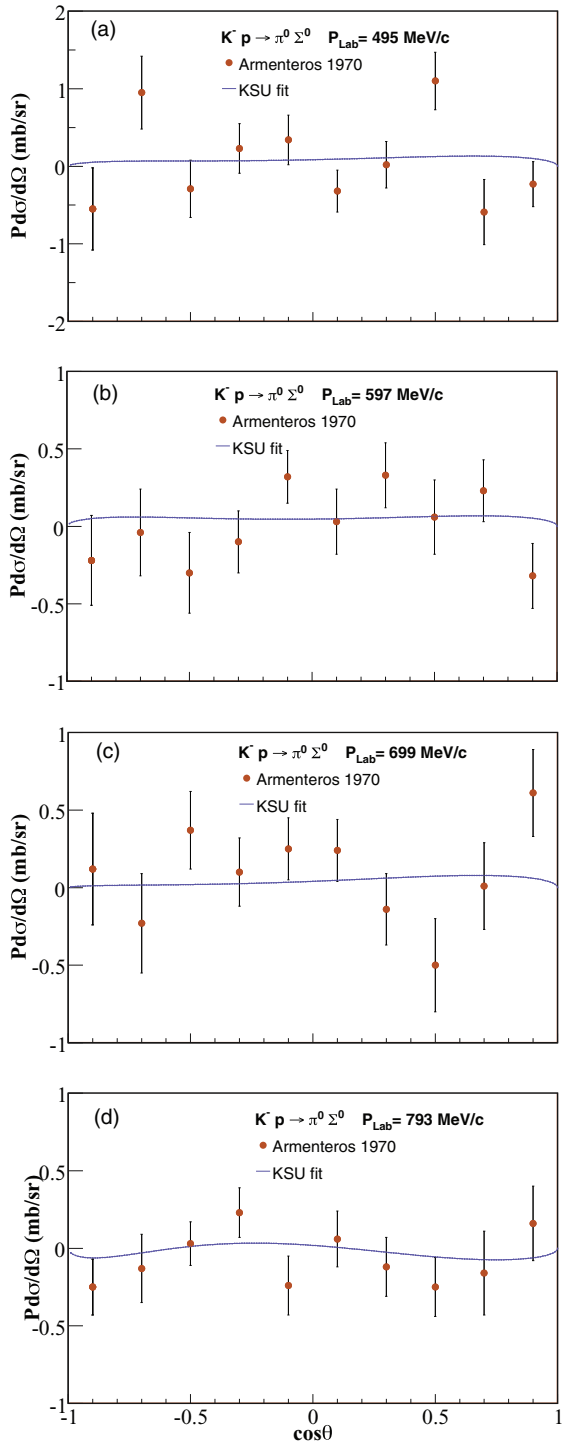

FIG. 14. (Color online) Representative results of our energy-dependent fit for the $K^- p \to \pi^0 \Sigma^0$ polarized cross section. Data are from Armenteros (1970) [10].

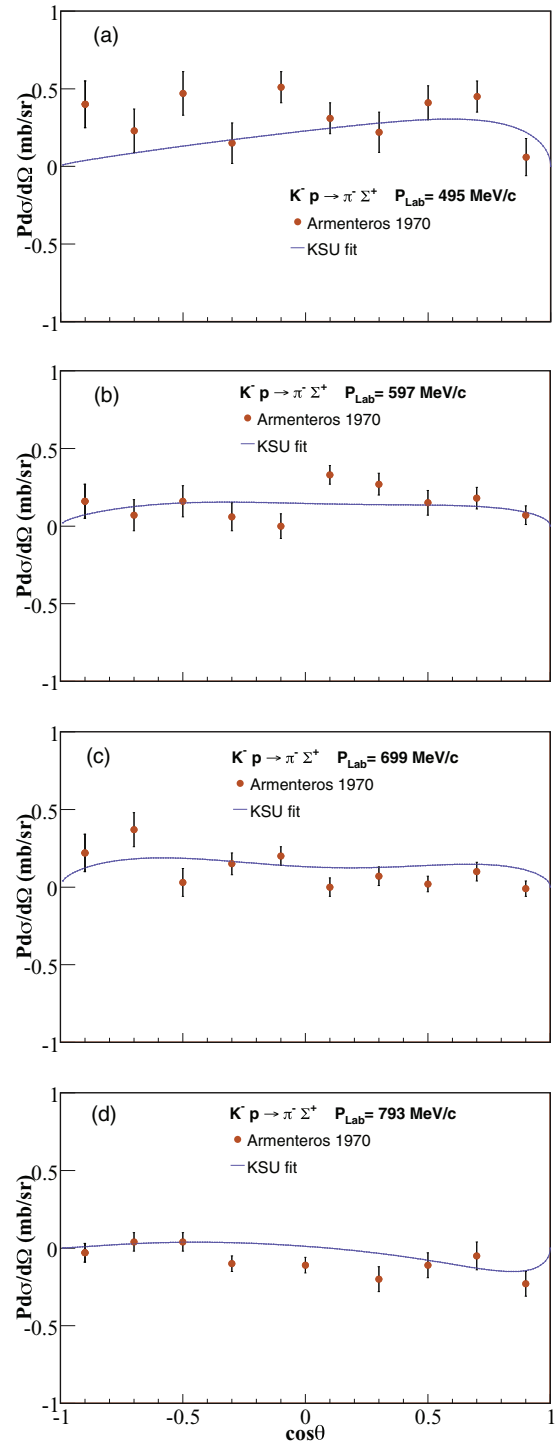

FIG. 15. (Color online) Representative results of our energy-dependent fit for the $K^- p \to \pi^- \Sigma^+$ polarized cross section. Data are from Armenteros (1970) [10].

single-energy analyses. At this stage, we successfully reduced our free amplitudes to include only S_{01}, S_{11}, and P_{01}. All other amplitudes were unchanged at the values from our last global fit, and slope parameters were again recalculated from the last global fit, and then held fixed in the single-energy fits.

III. RESULTS AND DISCUSSION

The final single-energy fits resulted in an excellent agreement with all observables ($d\sigma/d\Omega$, P, $P\,d\sigma/d\Omega$, and σ) yielding a fairly smooth set of partial-wave amplitudes within the energy range of our analysis. The energy-dependent

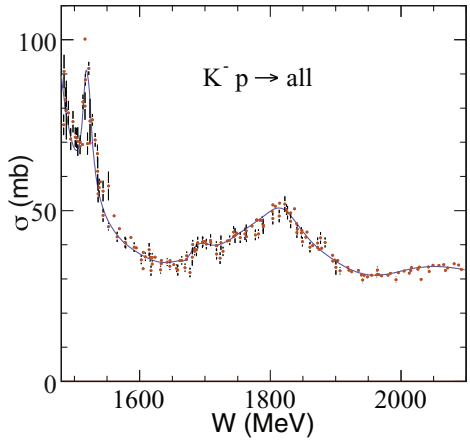

FIG. 16. (Color online) Total $K^- p$ cross section compared with the results of our energy-dependent fit. Data are from Baldini (1988) [22].

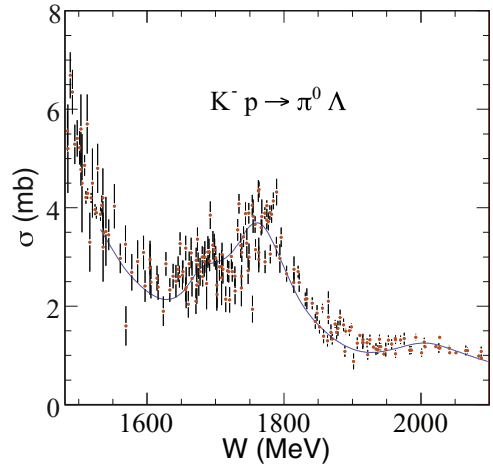

FIG. 18. (Color online) Integrated cross section for $K^- p \to \pi^0 \Lambda$ compared with the results of our energy-dependent fit. Data are from Baldini (1988) [22].

solutions were finally used to compare with the observable data. Figures 2–7 show representative energy-dependent results for the differential cross section of each $\overline{K}N$ reaction included in our single-energy fits. The cross sections are shown as a function of $\cos\theta$, where θ is the c.m. scattering angle of the meson. Figure 2 shows the comparison of differential cross section data for $K^- p \to K^- p$ with our energy-dependent solution at four laboratory momenta of 514, 935, 1165, and 1483 MeV/c. Although the data are from the 1960s and 1970s [2,10,20] they are in excellent agreement with our solution. For $K^- p \to \overline{K}^0 n$ (Fig. 3) the Crystal Ball data [12] with smaller error bars at $P_{\rm Lab} = 514$ and 750 MeV/c are well described by our solution at forward and backward angles with a slight under fitting at intermediate angles. The other data [18,19] at $P_{\rm Lab} = 1165$ and 1434 MeV/c with larger error bars are in good agreement with our energy-dependent solution. Similarly, Fig. 4 shows the excellent agreement between our solution and differential cross section data at $P_{\rm Lab} = 514$, 750, 1153, and 1465 MeV/c for $K^- p \to \pi^0 \Lambda$. Figure 5 shows a comparison of data from Refs. [10,14,18,24] with our solution for $K^- p \to \pi^+ \Sigma^-$. Except for some under-representation of data at $P_{\rm Lab} = 1245$ MeV/c we have an excellent agreement with the data. Figures 6 and 7 show an excellent agreement of our energy-dependent solution with the differential cross section data at various laboratory momenta of kaons for $K^- p \to \pi^0 \Sigma^0$ and $K^- p \to \pi^- \Sigma^+$, respectively.

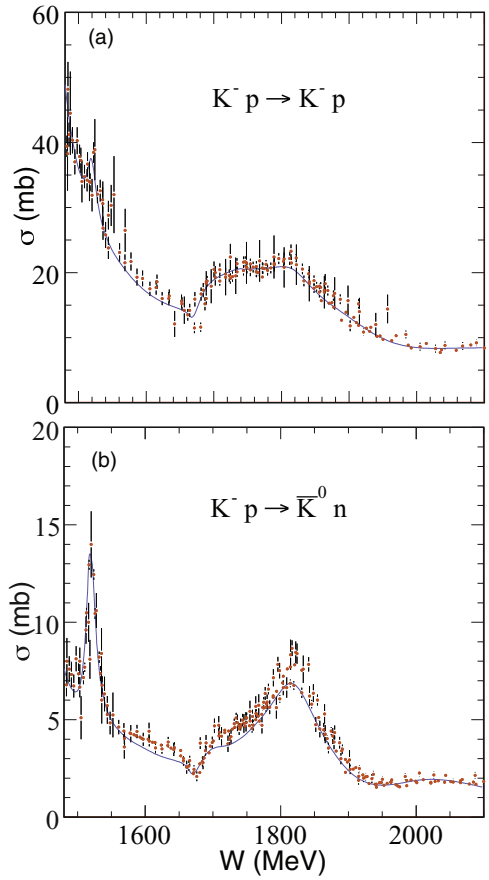

FIG. 17. (Color online) Integrated cross sections for $K^- p \to K^- p$ and $K^- p \to \overline{K}^0 n$ compared with the results of our energy-dependent fit. Data are from Baldini (1988) [22].

Figures 8, 9, 10, and 11 show representative energy-dependent fit results for the polarization in reactions $K^- p \to K^- p$, $K^- p \to \pi^0 \Lambda$, $K^- p \to \pi^0 \Sigma^0$, and $K^- p \to \pi^- \Sigma^+$, respectively. The polarizations are shown as a function of $\cos\theta$, where θ is the c.m. scattering angle of the meson. Figure 8 shows the excellent agreement of our energy-dependent solution with the $K^- p \to K^- p$ polarization at $P_{\rm Lab} = 1383$, 1483, 1584, and 1684 MeV/c from Ref. [20]. For $K^- p \to \pi^0 \Lambda$ (Fig. 9) our solution is in good agreement with the polarization data at $P_{\rm Lab} = 514$, 936, and 1165 MeV/c. Our solution also agrees well with the Crystal Ball data [12] at $P_{\rm Lab} = 714$ MeV/c at forward angles but there is a slight under-representation of data at backward angles. Similarly, Fig. 10 shows a very good agreement between our solution

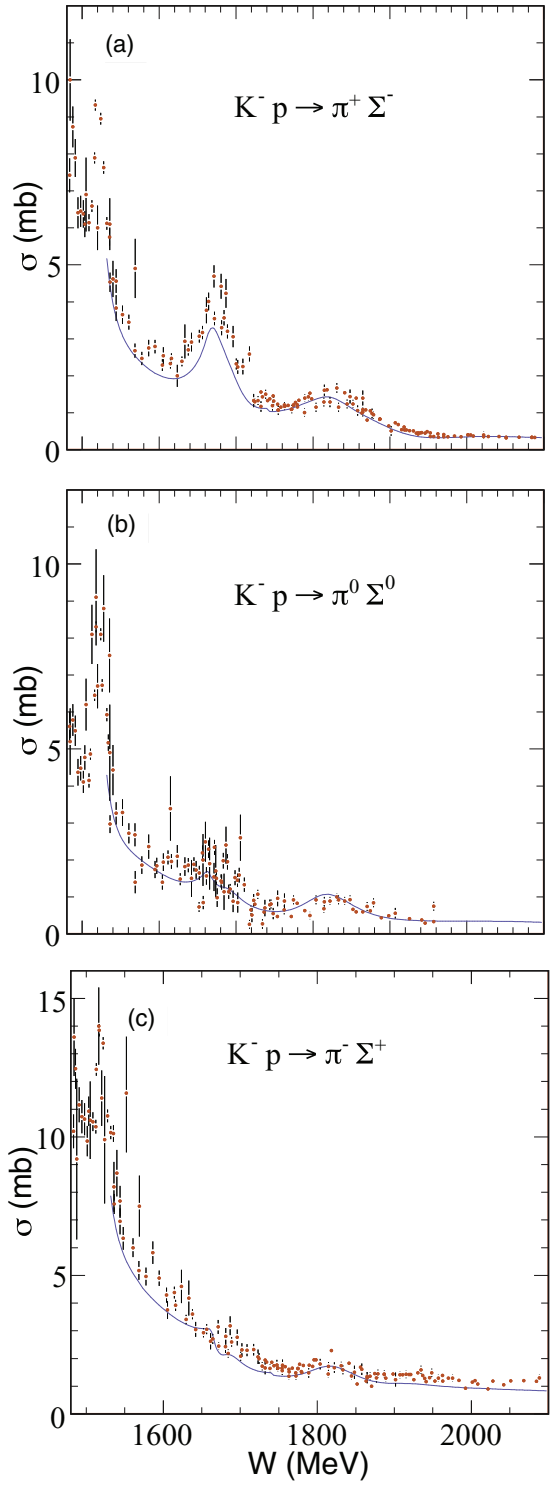

FIG. 19. (Color online) Integrated cross sections for $K^-p \to \pi^+\Sigma^-$, $K^-p \to \pi^0\Sigma^0$, and $K^-p \to \pi^-\Sigma^+$ compared with the results of our energy-dependent fit. Data are from Baldini (1988) [22].

and the $K^-p \to \pi^0\Sigma^0$ polarization data within the given uncertainties at $P_{\rm Lab} = 514$, 581, 687, and 750 MeV/c, all from the Crystal Ball Collaboration [12]. Finally, Fig. 11 shows a comparison of our solution with the $K^-p \to \pi^-\Sigma^+$ polarization data at $P_{\rm Lab} = 862$, 936, 1001, and 1125 MeV/c. Except for small forward angles at $P_{\rm Lab} = 1001$ MeV/c, we have good agreement with the data.

Figures 12, 13, 14, and 15 show representative energy-dependent fit results for the polarized cross section in reactions $K^-p \to K^-p$, $K^-p \to \pi^0\Lambda$, $K^-p \to \pi^0\Sigma^0$, and $K^-p \to \pi^-\Sigma^+$, respectively. The polarized cross sections are shown as a function of $\cos\theta$, where θ is the c.m. scattering angle of the meson. Within the uncertainties associated with the polarized cross section data our results are in good agreement with the data for these reactions.

Figure 16 shows our prediction for the total K^-p cross section. Figure 17 shows our predictions for the $K^-p \to K^-p$ and $K^-p \to \overline{K}^0n$ integrated cross sections, Fig. 18 shows our prediction for the $K^-p \to \pi^0\Lambda$ integrated cross section, and Fig. 19 shows our predictions for the $K^-p \to \pi^+\Sigma^-$, $K^-p \to \pi^0\Sigma^0$, and $K^-p \to \pi^-\Sigma^+$ integrated cross sections. Figures 18 and 19 do not show predictions for c.m. energies below 1540 MeV because it was not possible to obtain single-energy amplitudes in this region where only integrated cross-section data are available.

IV. SUMMARY AND CONCLUSIONS

We have investigated $\overline{K}N \to \overline{K}N$, $\overline{K}N \to \pi\Lambda$, and $\overline{K}N \to \pi\Sigma$ reactions through single-energy analyses constrained by a global unitary energy-dependent fit from threshold to a c.m. energy of 2.1 GeV. We found partial waves up to G waves necessary to describe the available data for the reactions. This work was motivated, in part, by the relatively recent measurements for $K^-p \to \overline{K}^0n$, $K^-p \to \pi^0\Lambda$, $K^-p \to \pi^0\Sigma^0$, and $K^-p \to \eta\Lambda$ by the Crystal Ball Collaboration. We were successful in describing these data in addition to older data from constrained single-energy analyses. The partial-wave amplitudes thus extracted were used in our global multichannel fit. A discussion of the resonance parameters from this global fit, which is the most comprehensive multichannel fit to date for $\overline{K}N$ scattering reactions, is presented in a separate publication [7].

ACKNOWLEDGMENT

This work was supported by the US Department of Energy Grant No. DE-FG02-01ER41194.

APPENDIX

Table IV lists the real and imaginary parts of the $\overline{K}N \to \overline{K}N$ amplitudes tabulated against the central bin energies. Similarly, Table V lists $\overline{K}N \to \pi\Lambda$ amplitudes and Table VI lists $\overline{K}N \to \pi\Sigma$ amplitudes. The values in these tables represent the final single-energy solutions that were used as input into our subsequent global energy-dependent fits for given partial waves. Plots of all amplitudes in Tables IV–VI are shown in Ref. [7]. The amplitudes are also available in the form of data files [34].

TABLE IV. Single-energy amplitudes for $\overline{K}N \to \overline{K}N$.

W_0	S_{01}		P_{01}		P_{03}	
(MeV)	Re(S_{01})	Im(S_{01})	Re(P_{01})	Im(P_{01})	Re(P_{03})	Im(P_{03})
1480	0.022 ± 0.037	0.686 ± 0.019	0.057 ± 0.039	0.006 ± 0.036	0.065 ± 0.035	0.005 ± 0.023
1500	0.031 ± 0.028	0.763 ± 0.013	0.098 ± 0.028	0.025 ± 0.027	0.067 ± 0.025	0.010 ± 0.016
1520	0.038 ± 0.091	0.615 ± 0.052	0.218 ± 0.083	0.034 ± 0.048	0.015 ± 0.050	0.016 ± 0.076
1540	0.046 ± 0.029	0.785 ± 0.018	0.210 ± 0.029	0.102 ± 0.025	0.082 ± 0.028	0.024 ± 0.021
1560	0.055 ± 0.025	0.778 ± 0.015	0.205 ± 0.025	0.229 ± 0.024	0.127 ± 0.024	0.033 ± 0.017
1580	0.051 ± 0.027	0.799 ± 0.017	0.186 ± 0.028	0.245 ± 0.026	0.160 ± 0.026	0.043 ± 0.019
1600	0.097 ± 0.029	0.773 ± 0.019	0.165 ± 0.030	0.317 ± 0.028	0.166 ± 0.027	0.052 ± 0.021
1620	0.109 ± 0.030	0.811 ± 0.018	0.173 ± 0.031	0.288 ± 0.029	0.216 ± 0.027	0.101 ± 0.020
1640	0.053 ± 0.028	0.816 ± 0.017	0.138 ± 0.029	0.341 ± 0.027	0.243 ± 0.024	0.096 ± 0.019
1660	0.087 ± 0.028	0.751 ± 0.015	0.167 ± 0.028	0.252 ± 0.027	0.225 ± 0.023	0.144 ± 0.018
1680	0.234 ± 0.025	0.708 ± 0.022	0.045 ± 0.026	0.402 ± 0.022	0.256 ± 0.020	0.074 ± 0.023
1700	0.268 ± 0.026	0.835 ± 0.020	−0.020 ± 0.025	0.385 ± 0.024	0.253 ± 0.023	0.208 ± 0.021
1720	0.228 ± 0.028	0.878 ± 0.023	−0.047 ± 0.027	0.347 ± 0.024	0.297 ± 0.024	0.136 ± 0.024
1740	0.163 ± 0.019	0.864 ± 0.016	−0.036 ± 0.020	0.286 ± 0.019	0.289 ± 0.019	0.272 ± 0.017
1760	0.080 ± 0.027	0.941 ± 0.019	−0.007 ± 0.022	0.352 ± 0.022	0.231 ± 0.022	0.256 ± 0.021
1780	0.032 ± 0.027	0.903 ± 0.022	−0.007 ± 0.022	0.352 ± 0.022	0.231 ± 0.022	0.256 ± 0.021
1800	−0.031 ± 0.028	0.923 ± 0.021	−0.007 ± 0.020	0.426 ± 0.025	0.281 ± 0.023	0.236 ± 0.022
1820	−0.122 ± 0.028	0.891 ± 0.021	−0.013 ± 0.020	0.456 ± 0.027	0.317 ± 0.025	0.307 ± 0.022
1840	−0.157 ± 0.026	0.836 ± 0.021	−0.054 ± 0.023	0.489 ± 0.026	0.362 ± 0.025	0.347 ± 0.021
1860	−0.194 ± 0.026	0.796 ± 0.022	−0.075 ± 0.024	0.471 ± 0.025	0.285 ± 0.022	0.439 ± 0.021
1880	−0.214 ± 0.025	0.729 ± 0.022	−0.016 ± 0.023	0.416 ± 0.024	0.226 ± 0.020	0.474 ± 0.021
1900	−0.262 ± 0.027	0.643 ± 0.025	0.014 ± 0.026	0.379 ± 0.024	0.125 ± 0.022	0.475 ± 0.023
1920	−0.215 ± 0.029	0.590 ± 0.029	0.035 ± 0.030	0.382 ± 0.027	0.119 ± 0.024	0.436 ± 0.026
1940	−0.186 ± 0.022	0.525 ± 0.022	0.048 ± 0.023	0.392 ± 0.019	0.137 ± 0.017	0.427 ± 0.018
1960	−0.134 ± 0.030	0.475 ± 0.031	0.053 ± 0.032	0.371 ± 0.027	0.130 ± 0.023	0.419 ± 0.029
1980	−0.043 ± 0.030	0.490 ± 0.032	0.069 ± 0.032	0.348 ± 0.034	0.132 ± 0.026	0.367 ± 0.030
2000	0.032 ± 0.028	0.496 ± 0.027	0.131 ± 0.028	0.368 ± 0.028	0.111 ± 0.023	0.431 ± 0.025
2020	0.050 ± 0.037	0.516 ± 0.036	0.139 ± 0.037	0.334 ± 0.038	0.085 ± 0.036	0.420 ± 0.034
2040	0.037 ± 0.037	0.494 ± 0.035	0.150 ± 0.037	0.353 ± 0.037	0.074 ± 0.035	0.383 ± 0.034
2060	0.082 ± 0.032	0.583 ± 0.030	0.157 ± 0.031	0.412 ± 0.032	0.049 ± 0.032	0.440 ± 0.029
2080	0.078 ± 0.029	0.616 ± 0.027	0.134 ± 0.028	0.454 ± 0.029	0.029 ± 0.028	0.449 ± 0.025
2100	0.057 ± 0.039	0.542 ± 0.033	0.134 ± 0.038	0.482 ± 0.035	0.010 ± 0.038	0.462 ± 0.031
2120	0.062 ± 0.029	0.650 ± 0.025	0.113 ± 0.027	0.526 ± 0.027	−0.008 ± 0.027	0.459 ± 0.025
2140	0.041 ± 0.035	0.651 ± 0.032	0.080 ± 0.034	0.553 ± 0.033	−0.026 ± 0.033	0.463 ± 0.030
2160	0.045 ± 0.091	0.440 ± 0.076	0.047 ± 0.091	0.443 ± 0.075	−0.045 ± 0.089	0.352 ± 0.073
2180	0.034 ± 0.025	0.670 ± 0.025	0.038 ± 0.025	0.525 ± 0.025	−0.062 ± 0.025	0.450 ± 0.025
W_0	D_{03}		D_{05}		F_{05}	
(MeV)	Re(D_{03})	Im(D_{03})	Re(D_{05})	Im(D_{05})	Re(F_{05})	Im(F_{05})
1480	0.032 ± 0.037	0.003 ± 0.034	0.004 ± 0.034	0.001 ± 0.025	0.000 ± 0.035	0.000 ± 0.018
1500	0.132 ± 0.021	0.032 ± 0.024	0.007 ± 0.021	0.002 ± 0.016	0.001 ± 0.021	0.000 ± 0.009
1520	0.032 ± 0.015	0.427 ± 0.030	0.010 ± 0.036	0.003 ± 0.046	0.002 ± 0.053	0.000 ± 0.051
1540	−0.164 ± 0.027	0.128 ± 0.021	0.014 ± 0.027	0.003 ± 0.018	0.003 ± 0.028	0.000 ± 0.022
1560	−0.137 ± 0.023	0.029 ± 0.022	0.019 ± 0.023	0.003 ± 0.016	0.006 ± 0.022	0.000 ± 0.021
1580	−0.093 ± 0.026	0.047 ± 0.024	0.024 ± 0.025	0.003 ± 0.018	0.011 ± 0.024	0.000 ± 0.023
1600	−0.060 ± 0.027	0.045 ± 0.026	0.030 ± 0.026	0.004 ± 0.020	0.017 ± 0.025	0.000 ± 0.024
1620	−0.038 ± 0.028	0.007 ± 0.027	0.037 ± 0.026	0.005 ± 0.019	0.025 ± 0.024	0.001 ± 0.026
1640	−0.004 ± 0.026	0.034 ± 0.025	0.044 ± 0.025	0.006 ± 0.019	0.036 ± 0.020	0.002 ± 0.023
1660	0.018 ± 0.024	0.075 ± 0.024	0.082 ± 0.022	0.007 ± 0.017	0.062 ± 0.017	0.004 ± 0.022
1680	−0.013 ± 0.021	0.242 ± 0.020	0.096 ± 0.020	0.009 ± 0.021	0.076 ± 0.015	0.007 ± 0.018
1700	−0.178 ± 0.020	0.216 ± 0.021	0.116 ± 0.020	0.012 ± 0.019	0.087 ± 0.017	0.014 ± 0.018
1720	−0.205 ± 0.024	0.251 ± 0.022	0.084 ± 0.024	0.017 ± 0.019	0.124 ± 0.023	0.027 ± 0.021
1740	−0.190 ± 0.018	0.133 ± 0.014	0.090 ± 0.016	0.023 ± 0.011	0.172 ± 0.017	0.048 ± 0.012
1760	−0.191 ± 0.020	0.154 ± 0.018	0.073 ± 0.014	0.033 ± 0.014	0.292 ± 0.019	0.066 ± 0.015
1780	−0.202 ± 0.019	0.099 ± 0.021	0.100 ± 0.017	0.046 ± 0.017	0.359 ± 0.020	0.212 ± 0.014
1800	−0.161 ± 0.020	0.039 ± 0.021	0.097 ± 0.020	0.071 ± 0.015	0.268 ± 0.017	0.431 ± 0.012
1820	−0.067 ± 0.022	0.037 ± 0.019	0.092 ± 0.021	0.075 ± 0.015	0.102 ± 0.015	0.578 ± 0.014

TABLE IV. (*Continued*.)

W_0	D_{03}		D_{05}		F_{05}	
(MeV)	Re(D_{03})	Im(D_{03})	Re(D_{05})	Im(D_{05})	Re(F_{05})	Im(F_{05})
1840	−0.086 ± 0.022	0.056 ± 0.018	0.070 ± 0.020	0.033 ± 0.016	−0.129 ± 0.018	0.509 ± 0.014
1860	−0.043 ± 0.022	0.033 ± 0.020	0.081 ± 0.019	0.066 ± 0.018	−0.209 ± 0.018	0.376 ± 0.016
1880	−0.041 ± 0.021	0.081 ± 0.020	0.119 ± 0.017	0.063 ± 0.019	−0.217 ± 0.016	0.290 ± 0.016
1900	−0.027 ± 0.023	0.124 ± 0.023	0.111 ± 0.019	0.055 ± 0.023	−0.222 ± 0.019	0.218 ± 0.018
1920	−0.015 ± 0.027	0.116 ± 0.026	0.125 ± 0.022	0.066 ± 0.027	−0.225 ± 0.023	0.175 ± 0.022
1940	−0.007 ± 0.021	0.132 ± 0.019	0.118 ± 0.015	0.060 ± 0.020	−0.193 ± 0.016	0.156 ± 0.015
1960	−0.001 ± 0.029	0.140 ± 0.025	0.136 ± 0.022	0.111 ± 0.029	−0.190 ± 0.022	0.158 ± 0.023
1980	0.000 ± 0.031	0.154 ± 0.031	0.093 ± 0.024	0.107 ± 0.030	−0.188 ± 0.024	0.121 ± 0.030
2000	−0.001 ± 0.027	0.172 ± 0.026	0.162 ± 0.021	0.130 ± 0.026	−0.205 ± 0.021	0.121 ± 0.026
2020	−0.007 ± 0.037	0.200 ± 0.035	0.147 ± 0.032	0.120 ± 0.035	−0.210 ± 0.029	0.138 ± 0.035
2040	−0.016 ± 0.037	0.207 ± 0.034	0.091 ± 0.033	0.170 ± 0.034	−0.207 ± 0.029	0.121 ± 0.034
2060	−0.029 ± 0.031	0.223 ± 0.030	0.160 ± 0.027	0.178 ± 0.029	−0.190 ± 0.026	0.143 ± 0.030
2080	−0.044 ± 0.028	0.238 ± 0.027	0.142 ± 0.025	0.176 ± 0.026	−0.173 ± 0.025	0.141 ± 0.027
2100	−0.093 ± 0.037	0.221 ± 0.034	0.145 ± 0.033	0.198 ± 0.031	−0.153 ± 0.034	0.152 ± 0.034
2120	−0.126 ± 0.026	0.257 ± 0.026	0.114 ± 0.023	0.201 ± 0.024	−0.182 ± 0.023	0.137 ± 0.025
2140	−0.111 ± 0.032	0.271 ± 0.032	0.086 ± 0.030	0.227 ± 0.030	−0.165 ± 0.029	0.142 ± 0.031
2160	0.001 ± 0.090	0.171 ± 0.075	−0.020 ± 0.090	0.218 ± 0.070	−0.055 ± 0.088	0.204 ± 0.075
2180	−0.126 ± 0.025	0.245 ± 0.025	0.062 ± 0.025	0.224 ± 0.025	−0.170 ± 0.025	0.113 ± 0.025

W_0	F_{07}		G_{07}	
(MeV)	Re(G_{07})	Im(G_{07})	Re(G_{07})	Im(G_{07})
1480	0.000 ± 0.032	0.000 ± 0.025	0.000 ± 0.021	0.000 ± 0.025
1500	0.000 ± 0.014	0.000 ± 0.025	0.000 ± 0.017	0.000 ± 0.005
1520	0.000 ± 0.026	0.000 ± 0.014	0.000 ± 0.043	0.000 ± 0.032
1540	0.001 ± 0.018	0.000 ± 0.017	0.000 ± 0.026	0.000 ± 0.011
1560	0.001 ± 0.017	0.000 ± 0.017	0.000 ± 0.019	0.000 ± 0.011
1580	0.002 ± 0.022	0.000 ± 0.019	0.001 ± 0.016	0.000 ± 0.012
1600	0.003 ± 0.023	0.000 ± 0.019	0.001 ± 0.016	0.000 ± 0.013
1620	0.003 ± 0.022	0.000 ± 0.019	0.001 ± 0.010	0.000 ± 0.010
1640	0.005 ± 0.021	0.000 ± 0.018	0.002 ± 0.008	0.000 ± 0.010
1660	0.006 ± 0.018	0.000 ± 0.018	0.003 ± 0.011	0.000 ± 0.009
1680	0.007 ± 0.013	0.000 ± 0.012	0.005 ± 0.009	0.000 ± 0.012
1700	0.009 ± 0.014	0.000 ± 0.013	0.007 ± 0.017	0.000 ± 0.012
1720	0.011 ± 0.017	0.000 ± 0.015	0.009 ± 0.019	0.000 ± 0.014
1740	0.012 ± 0.011	0.000 ± 0.011	0.012 ± 0.014	0.000 ± 0.009
1760	0.014 ± 0.011	0.000 ± 0.014	0.016 ± 0.017	0.001 ± 0.011
1780	0.016 ± 0.011	0.000 ± 0.015	0.021 ± 0.018	0.001 ± 0.012
1800	0.019 ± 0.017	0.000 ± 0.014	0.027 ± 0.016	0.001 ± 0.013
1820	0.021 ± 0.020	0.001 ± 0.011	0.034 ± 0.016	0.002 ± 0.015
1840	0.023 ± 0.019	0.001 ± 0.011	0.043 ± 0.016	0.003 ± 0.013
1860	0.026 ± 0.017	0.001 ± 0.013	0.041 ± 0.015	0.005 ± 0.012
1880	0.029 ± 0.013	0.002 ± 0.013	0.085 ± 0.012	0.010 ± 0.009
1900	0.033 ± 0.014	0.002 ± 0.016	0.080 ± 0.012	0.017 ± 0.011
1920	0.037 ± 0.015	0.004 ± 0.019	0.116 ± 0.018	0.029 ± 0.014
1940	0.041 ± 0.012	0.006 ± 0.014	0.139 ± 0.011	0.046 ± 0.010
1960	0.045 ± 0.017	0.009 ± 0.020	0.138 ± 0.018	0.066 ± 0.015
1980	0.048 ± 0.021	0.015 ± 0.025	0.174 ± 0.022	0.160 ± 0.019
2000	0.049 ± 0.021	0.022 ± 0.022	0.140 ± 0.020	0.163 ± 0.021
2020	0.046 ± 0.033	0.028 ± 0.029	0.151 ± 0.028	0.199 ± 0.027
2040	0.042 ± 0.032	0.030 ± 0.027	0.124 ± 0.027	0.269 ± 0.021
2060	0.038 ± 0.029	0.031 ± 0.025	0.090 ± 0.024	0.234 ± 0.022
2080	0.036 ± 0.026	0.030 ± 0.021	0.069 ± 0.024	0.253 ± 0.021
2100	0.035 ± 0.035	0.029 ± 0.027	0.020 ± 0.032	0.310 ± 0.022
2120	0.035 ± 0.024	0.028 ± 0.021	−0.008 ± 0.019	0.268 ± 0.016
2140	0.035 ± 0.031	0.027 ± 0.027	−0.032 ± 0.028	0.258 ± 0.022
2160	0.035 ± 0.087	0.027 ± 0.046	0.049 ± 0.085	0.234 ± 0.057
2180	0.036 ± 0.025	0.026 ± 0.025	−0.065 ± 0.025	0.235 ± 0.025

TABLE IV. (*Continued*.)

W_0	S_{11}		P_{11}		P_{13}	
(MeV)	Re(S_{11})	Im(S_{11})	Re(P_{11})	Im(P_{11})	Re(P_{13})	Im(P_{13})
1480	0.232 ± 0.037	0.329 ± 0.019	0.006 ± 0.039	0.020 ± 0.036	−0.034 ± 0.035	0.008 ± 0.023
1500	0.191 ± 0.027	0.352 ± 0.012	0.038 ± 0.027	0.022 ± 0.027	−0.040 ± 0.024	0.009 ± 0.016
1520	0.125 ± 0.053	0.360 ± 0.037	0.168 ± 0.049	0.030 ± 0.061	−0.041 ± 0.039	0.010 ± 0.039
1540	0.118 ± 0.029	0.385 ± 0.014	0.029 ± 0.029	0.042 ± 0.025	−0.036 ± 0.028	0.011 ± 0.019
1560	0.178 ± 0.025	0.357 ± 0.015	0.085 ± 0.025	0.083 ± 0.023	−0.028 ± 0.024	0.010 ± 0.017
1580	0.199 ± 0.028	0.339 ± 0.017	0.084 ± 0.028	0.082 ± 0.026	−0.020 ± 0.025	0.013 ± 0.019
1600	0.251 ± 0.029	0.331 ± 0.019	0.069 ± 0.030	0.061 ± 0.027	−0.014 ± 0.027	0.020 ± 0.021
1620	0.197 ± 0.030	0.381 ± 0.018	0.026 ± 0.030	0.035 ± 0.029	−0.007 ± 0.027	0.028 ± 0.021
1640	0.194 ± 0.029	0.393 ± 0.017	0.042 ± 0.029	0.063 ± 0.027	0.001 ± 0.025	0.035 ± 0.019
1660	0.262 ± 0.028	0.350 ± 0.015	0.031 ± 0.027	0.156 ± 0.027	0.008 ± 0.023	0.040 ± 0.019
1680	0.368 ± 0.025	0.365 ± 0.022	0.021 ± 0.026	0.140 ± 0.022	0.016 ± 0.020	0.046 ± 0.020
1700	0.372 ± 0.026	0.420 ± 0.021	0.012 ± 0.026	0.156 ± 0.024	0.024 ± 0.022	−0.038 ± 0.021
1720	0.385 ± 0.027	0.462 ± 0.023	0.005 ± 0.028	0.097 ± 0.024	0.031 ± 0.025	0.083 ± 0.024
1740	0.273 ± 0.019	0.639 ± 0.016	0.006 ± 0.021	0.024 ± 0.019	0.039 ± 0.019	0.034 ± 0.016
1760	0.255 ± 0.027	0.633 ± 0.019	0.019 ± 0.022	0.063 ± 0.023	0.047 ± 0.022	0.048 ± 0.020
1780	0.148 ± 0.028	0.674 ± 0.022	0.044 ± 0.022	0.094 ± 0.025	0.062 ± 0.023	0.102 ± 0.023
1800	0.097 ± 0.029	0.666 ± 0.022	0.134 ± 0.020	0.105 ± 0.026	0.076 ± 0.025	0.102 ± 0.022
1820	0.055 ± 0.028	0.651 ± 0.022	0.130 ± 0.023	0.117 ± 0.025	0.093 ± 0.026	0.120 ± 0.019
1840	0.060 ± 0.026	0.662 ± 0.021	0.133 ± 0.023	0.138 ± 0.023	0.095 ± 0.022	0.144 ± 0.018
1860	0.027 ± 0.027	0.696 ± 0.022	0.088 ± 0.024	0.176 ± 0.025	0.072 ± 0.022	0.157 ± 0.020
1880	−0.034 ± 0.026	0.723 ± 0.022	0.062 ± 0.023	0.174 ± 0.024	0.082 ± 0.021	0.165 ± 0.020
1900	−0.152 ± 0.027	0.709 ± 0.025	0.090 ± 0.026	0.175 ± 0.025	0.062 ± 0.022	0.190 ± 0.022
1920	−0.244 ± 0.030	0.668 ± 0.029	0.091 ± 0.030	0.202 ± 0.028	0.061 ± 0.025	0.210 ± 0.026
1940	−0.305 ± 0.022	0.628 ± 0.022	0.088 ± 0.023	0.182 ± 0.021	0.045 ± 0.017	0.243 ± 0.019
1960	−0.371 ± 0.030	0.550 ± 0.031	0.069 ± 0.032	0.209 ± 0.029	0.037 ± 0.024	0.244 ± 0.029
1980	−0.408 ± 0.032	0.476 ± 0.032	0.043 ± 0.032	0.260 ± 0.034	0.027 ± 0.028	0.272 ± 0.029
2000	−0.334 ± 0.028	0.426 ± 0.027	0.030 ± 0.028	0.228 ± 0.028	0.014 ± 0.025	0.265 ± 0.024
2020	−0.292 ± 0.038	0.389 ± 0.035	0.021 ± 0.037	0.208 ± 0.038	0.001 ± 0.036	0.284 ± 0.033
2040	−0.296 ± 0.038	0.298 ± 0.035	0.014 ± 0.037	0.228 ± 0.038	−0.011 ± 0.035	0.287 ± 0.033
2060	−0.187 ± 0.033	0.314 ± 0.030	0.010 ± 0.031	0.231 ± 0.032	−0.021 ± 0.032	0.280 ± 0.028
2080	−0.150 ± 0.029	0.331 ± 0.027	0.006 ± 0.028	0.234 ± 0.029	−0.030 ± 0.028	0.272 ± 0.025
2100	−0.173 ± 0.039	0.257 ± 0.034	0.005 ± 0.038	0.231 ± 0.036	−0.037 ± 0.038	0.277 ± 0.030
2120	−0.109 ± 0.029	0.376 ± 0.025	0.010 ± 0.027	0.246 ± 0.028	−0.039 ± 0.027	0.277 ± 0.024
2140	−0.128 ± 0.035	0.372 ± 0.032	0.018 ± 0.034	0.230 ± 0.034	−0.039 ± 0.033	0.252 ± 0.029
2160	−0.098 ± 0.091	0.439 ± 0.076	0.023 ± 0.091	0.271 ± 0.075	−0.038 ± 0.089	0.346 ± 0.073
2180	−0.115 ± 0.025	0.428 ± 0.025	0.025 ± 0.025	0.208 ± 0.025	−0.040 ± 0.025	0.263 ± 0.025
W_0	D_{13}		D_{15}		F_{15}	
(MeV)	Re(D_{13})	Im(D_{13})	Re(D_{15})	Im(D_{15})	Re(F_{15})	Im(F_{15})
1480	0.000 ± 0.025	0.000 ± 0.025	0.004 ± 0.033	0.000 ± 0.018	0.000 ± 0.025	0.000 ± 0.025
1500	0.000 ± 0.025	0.000 ± 0.025	0.008 ± 0.018	0.000 ± 0.009	0.000 ± 0.025	0.000 ± 0.025
1520	0.000 ± 0.025	0.000 ± 0.025	0.015 ± 0.031	0.001 ± 0.014	0.000 ± 0.025	0.000 ± 0.025
1540	0.000 ± 0.025	0.000 ± 0.025	0.024 ± 0.020	0.001 ± 0.011	0.000 ± 0.025	0.000 ± 0.025
1560	0.002 ± 0.023	0.014 ± 0.022	0.035 ± 0.018	0.002 ± 0.016	0.000 ± 0.025	0.000 ± 0.025
1580	0.007 ± 0.026	0.023 ± 0.024	0.048 ± 0.023	0.005 ± 0.018	0.000 ± 0.025	0.000 ± 0.025
1600	0.014 ± 0.028	0.034 ± 0.026	0.069 ± 0.026	0.008 ± 0.019	0.000 ± 0.025	0.000 ± 0.025
1620	0.023 ± 0.028	0.048 ± 0.027	0.068 ± 0.027	0.014 ± 0.018	0.000 ± 0.025	0.000 ± 0.025
1640	0.032 ± 0.026	0.030 ± 0.025	0.080 ± 0.025	0.023 ± 0.017	0.000 ± 0.025	0.000 ± 0.025
1660	0.026 ± 0.024	0.078 ± 0.024	0.121 ± 0.024	0.038 ± 0.017	0.000 ± 0.025	0.000 ± 0.025
1680	−0.019 ± 0.023	0.098 ± 0.020	0.138 ± 0.020	0.057 ± 0.014	0.000 ± 0.025	0.000 ± 0.025
1700	−0.029 ± 0.022	0.100 ± 0.021	0.184 ± 0.021	0.130 ± 0.017	0.000 ± 0.025	0.000 ± 0.025
1720	−0.017 ± 0.024	0.020 ± 0.022	0.213 ± 0.021	0.185 ± 0.016	0.012 ± 0.022	0.001 ± 0.021
1740	−0.005 ± 0.019	0.017 ± 0.014	0.156 ± 0.015	0.333 ± 0.011	0.015 ± 0.015	0.002 ± 0.012
1760	0.004 ± 0.021	0.071 ± 0.018	0.103 ± 0.012	0.352 ± 0.015	0.018 ± 0.018	0.003 ± 0.015
1780	0.010 ± 0.020	0.072 ± 0.021	−0.002 ± 0.012	0.384 ± 0.017	0.022 ± 0.018	0.004 ± 0.015
1800	0.016 ± 0.020	0.090 ± 0.022	−0.124 ± 0.018	0.338 ± 0.014	0.026 ± 0.016	0.006 ± 0.013
1820	0.022 ± 0.022	0.060 ± 0.020	−0.163 ± 0.020	0.288 ± 0.013	0.031 ± 0.014	0.009 ± 0.013

TABLE IV. (*Continued*.)

W_0	D_{13}		D_{15}		F_{15}	
(MeV)	Re(D_{13})	Im(D_{13})	Re(D_{15})	Im(D_{15})	Re(F_{15})	Im(F_{15})
1840	0.026 ± 0.021	0.064 ± 0.019	-0.134 ± 0.020	0.237 ± 0.014	0.036 ± 0.018	0.014 ± 0.013
1860	0.028 ± 0.022	0.080 ± 0.020	-0.149 ± 0.019	0.195 ± 0.017	0.041 ± 0.018	0.021 ± 0.016
1880	0.030 ± 0.021	0.101 ± 0.020	-0.164 ± 0.017	0.138 ± 0.018	0.044 ± 0.016	0.030 ± 0.015
1900	0.033 ± 0.023	0.125 ± 0.023	-0.123 ± 0.020	0.124 ± 0.021	0.044 ± 0.019	0.040 ± 0.018
1920	0.036 ± 0.028	0.116 ± 0.027	-0.089 ± 0.022	0.119 ± 0.026	0.040 ± 0.023	0.048 ± 0.022
1940	0.040 ± 0.020	0.098 ± 0.019	-0.083 ± 0.015	0.110 ± 0.019	0.036 ± 0.016	0.050 ± 0.015
1960	0.042 ± 0.02	0.135 ± 0.025	-0.057 ± 0.022	0.077 ± 0.027	0.034 ± 0.022	0.039 ± 0.023
1980	0.041 ± 0.031	0.103 ± 0.032	-0.062 ± 0.024	0.102 ± 0.030	0.033 ± 0.023	0.087 ± 0.030
2000	0.039 ± 0.027	0.127 ± 0.026	-0.010 ± 0.021	0.099 ± 0.026	0.032 ± 0.021	0.064 ± 0.025
2020	0.038 ± 0.037	0.141 ± 0.035	0.012 ± 0.032	0.116 ± 0.035	0.029 ± 0.029	0.057 ± 0.035
2040	0.037 ± 0.037	0.154 ± 0.034	-0.007 ± 0.033	0.132 ± 0.034	0.024 ± 0.028	0.048 ± 0.034
2060	0.037 ± 0.031	0.134 ± 0.030	-0.045 ± 0.027	0.123 ± 0.029	0.015 ± 0.026	0.100 ± 0.030
2080	0.037 ± 0.028	0.136 ± 0.027	-0.041 ± 0.025	0.109 ± 0.026	0.003 ± 0.025	0.105 ± 0.027
2100	0.038 ± 0.037	0.101 ± 0.035	-0.037 ± 0.033	0.120 ± 0.031	-0.009 ± 0.033	0.104 ± 0.033
2120	0.040 ± 0.026	0.144 ± 0.026	-0.034 ± 0.023	0.121 ± 0.024	-0.020 ± 0.023	0.110 ± 0.025
2140	0.044 ± 0.032	0.140 ± 0.032	-0.033 ± 0.030	0.126 ± 0.030	-0.030 ± 0.029	0.109 ± 0.031
2160	0.048 ± 0.090	0.093 ± 0.076	-0.037 ± 0.090	0.141 ± 0.070	-0.037 ± 0.087	0.121 ± 0.074
2180	0.050 ± 0.025	0.137 ± 0.025	-0.046 ± 0.025	0.141 ± 0.025	-0.043 ± 0.025	0.083 ± 0.025
W_0	F_{17}		G_{17}			
(MeV)	Re(F_{17})	Im(F_{17})	Re(G_{17})	Im(G_{17})		
1480	0.000 ± 0.031	0.000 ± 0.014	0.000	0.000		
1500	0.000 ± 0.013	0.000 ± 0.008	0.000	0.000		
1520	0.001 ± 0.026	0.000 ± 0.015	0.000	0.000		
1540	0.002 ± 0.015	0.000 ± 0.009	0.000	0.000		
1560	0.003 ± 0.016	0.000 ± 0.008	0.001	0.000		
1580	0.005 ± 0.020	0.000 ± 0.009	0.001	0.000		
1600	0.007 ± 0.023	0.000 ± 0.010	0.002	0.001		
1620	0.009 ± 0.020	0.000 ± 0.010	0.003	0.002		
1640	0.012 ± 0.020	0.000 ± 0.009	0.003	0.003		
1660	0.016 ± 0.018	0.000 ± 0.009	0.003	0.004		
1680	0.020 ± 0.013	0.001 ± 0.009	0.003	0.004		
1700	0.024 ± 0.012	0.001 ± 0.010	0.003	0.004		
1720	0.029 ± 0.015	0.002 ± 0.016	0.003	0.005		
1740	0.035 ± 0.010	0.003 ± 0.011	0.004	0.005		
1760	0.041 ± 0.011	0.004 ± 0.014	0.004	0.005		
1780	0.047 ± 0.012	0.006 ± 0.017	0.006	0.006		
1800	0.025 ± 0.017	0.008 ± 0.015	0.007	0.006		
1820	0.058 ± 0.020	0.011 ± 0.013	0.008	0.007		
1840	0.097 ± 0.018	0.014 ± 0.012	0.010	0.008		
1860	0.108 ± 0.017	0.017 ± 0.014	0.012	0.009		
1880	0.092 ± 0.014	0.022 ± 0.013	0.015	0.010		
1900	0.114 ± 0.014	0.029 ± 0.017	0.018	0.012		
1920	0.118 ± 0.016	0.040 ± 0.019	0.021	0.014		
1940	0.114 ± 0.011	0.064 ± 0.014	0.024	0.017		
1960	0.137 ± 0.017	0.093 ± 0.019	0.028	0.020		
1980	0.109 ± 0.022	0.071 ± 0.026	0.032	0.024		
2000	0.108 ± 0.021	0.126 ± 0.023	0.037	0.029		
2020	0.094 ± 0.033	0.164 ± 0.031	0.041	0.036		
2040	0.055 ± 0.032	0.177 ± 0.030	0.046	0.043		
2060	0.031 ± 0.029	0.177 ± 0.026	0.056	0.052		
2080	0.009 ± 0.026	0.202 ± 0.023	0.068	0.053		
2100	-0.007 ± 0.035	0.168 ± 0.029	0.029	0.105		
2120	-0.016 ± 0.024	0.155 ± 0.022	0.058	0.093		
2140	-0.022 ± 0.030	0.139 ± 0.028	0.045	0.117		
2160	-0.025 ± 0.087	0.187 ± 0.050	0.033	0.185		
2180	-0.028 ± 0.025	0.117 ± 0.025	0.017	0.137		

TABLE V. Single-energy amplitudes for $\overline{K}N \to \pi\Lambda$.

W_0	S_{11}		P_{11}		P_{13}	
(MeV)	Re(S_{11})	Im(S_{11})	Re(P_{11})	Im(P_{11})	Re(P_{13})	Im(P_{13})
1480	-0.218 ± 0.035	-0.108 ± 0.035	-0.055 ± 0.035	-0.020 ± 0.035	-0.071 ± 0.035	-0.016 ± 0.035
1500	-0.209 ± 0.035	-0.119 ± 0.035	-0.071 ± 0.035	-0.031 ± 0.035	-0.076 ± 0.035	-0.019 ± 0.035
1520	-0.206 ± 0.035	-0.121 ± 0.035	-0.094 ± 0.035	-0.049 ± 0.035	-0.076 ± 0.035	-0.019 ± 0.035
1540	-0.237 ± 0.023	-0.149 ± 0.031	-0.093 ± 0.031	-0.098 ± 0.031	-0.058 ± 0.019	-0.019 ± 0.025
1560	-0.239 ± 0.025	-0.165 ± 0.033	-0.079 ± 0.032	-0.060 ± 0.029	-0.042 ± 0.020	-0.016 ± 0.029
1580	-0.252 ± 0.027	-0.216 ± 0.031	-0.042 ± 0.031	-0.039 ± 0.032	-0.049 ± 0.021	-0.012 ± 0.028
1600	-0.239 ± 0.030	-0.222 ± 0.031	-0.049 ± 0.031	-0.067 ± 0.034	-0.031 ± 0.023	-0.005 ± 0.030
1620	-0.263 ± 0.035	-0.172 ± 0.045	-0.104 ± 0.041	-0.143 ± 0.040	-0.013 ± 0.024	0.005 ± 0.046
1640	-0.279 ± 0.020	-0.082 ± 0.034	-0.190 ± 0.030	-0.153 ± 0.026	0.001 ± 0.010	0.019 ± 0.030
1660	-0.298 ± 0.021	-0.130 ± 0.040	-0.136 ± 0.033	-0.116 ± 0.030	0.010 ± 0.015	0.031 ± 0.033
1680	-0.307 ± 0.023	-0.162 ± 0.039	-0.140 ± 0.028	-0.104 ± 0.029	0.015 ± 0.015	0.042 ± 0.033
1700	-0.279 ± 0.029	-0.073 ± 0.038	-0.179 ± 0.025	0.011 ± 0.037	0.017 ± 0.017	0.050 ± 0.038
1720	-0.179 ± 0.026	-0.105 ± 0.030	-0.170 ± 0.024	-0.108 ± 0.028	0.019 ± 0.024	0.062 ± 0.024
1740	-0.167 ± 0.027	-0.074 ± 0.031	-0.183 ± 0.025	-0.107 ± 0.028	0.019 ± 0.025	0.089 ± 0.026
1760	-0.167 ± 0.034	-0.012 ± 0.030	-0.173 ± 0.029	-0.094 ± 0.031	0.020 ± 0.031	0.074 ± 0.031
1780	-0.192 ± 0.032	0.006 ± 0.027	-0.181 ± 0.027	-0.113 ± 0.029	0.022 ± 0.032	0.072 ± 0.026
1800	-0.211 ± 0.031	0.012 ± 0.028	-0.209 ± 0.028	-0.112 ± 0.029	0.024 ± 0.032	0.071 ± 0.024
1820	-0.148 ± 0.030	0.015 ± 0.023	-0.208 ± 0.025	-0.022 ± 0.027	0.028 ± 0.032	0.052 ± 0.022
1840	-0.139 ± 0.028	0.015 ± 0.024	-0.208 ± 0.025	-0.082 ± 0.027	0.036 ± 0.029	0.043 ± 0.019
1860	-0.134 ± 0.041	0.013 ± 0.036	-0.199 ± 0.034	-0.066 ± 0.041	0.045 ± 0.036	0.044 ± 0.026
1880	-0.133 ± 0.031	0.014 ± 0.028	-0.198 ± 0.025	-0.083 ± 0.033	0.038 ± 0.025	0.049 ± 0.018
1900	-0.109 ± 0.038	0.017 ± 0.033	-0.194 ± 0.031	-0.059 ± 0.038	0.067 ± 0.027	0.045 ± 0.025
1920	-0.119 ± 0.027	0.028 ± 0.029	-0.233 ± 0.026	-0.074 ± 0.032	0.070 ± 0.025	0.041 ± 0.019
1940	-0.100 ± 0.025	0.047 ± 0.020	-0.204 ± 0.018	-0.051 ± 0.029	0.053 ± 0.016	0.038 ± 0.015
1960	-0.107 ± 0.025	0.095 ± 0.023	-0.204 ± 0.017	-0.001 ± 0.034	0.046 ± 0.018	0.035 ± 0.017
1980	-0.097 ± 0.030	0.065 ± 0.028	-0.191 ± 0.030	-0.052 ± 0.035	0.048 ± 0.028	0.035 ± 0.028
2000	-0.107 ± 0.042	0.174 ± 0.029	-0.150 ± 0.033	-0.027 ± 0.037	0.030 ± 0.033	0.037 ± 0.024
2020	-0.063 ± 0.035	0.080 ± 0.035	-0.129 ± 0.035	-0.052 ± 0.035	0.079 ± 0.035	0.038 ± 0.035
2040	-0.089 ± 0.035	0.145 ± 0.035	-0.185 ± 0.035	-0.048 ± 0.035	0.041 ± 0.035	0.038 ± 0.035
2060	-0.164 ± 0.057	0.129 ± 0.045	-0.228 ± 0.052	-0.044 ± 0.053	0.050 ± 0.047	0.039 ± 0.042
2080	-0.120 ± 0.067	0.117 ± 0.046	-0.209 ± 0.053	-0.039 ± 0.060	0.047 ± 0.052	0.039 ± 0.048
2100	-0.075 ± 0.035	0.010 ± 0.035	-0.058 ± 0.035	-0.036 ± 0.035	0.046 ± 0.035	0.038 ± 0.035
2120	-0.122 ± 0.072	0.141 ± 0.047	-0.205 ± 0.058	-0.038 ± 0.065	0.046 ± 0.045	0.037 ± 0.049
2140	-0.113 ± 0.035	0.135 ± 0.035	-0.164 ± 0.035	-0.040 ± 0.035	0.045 ± 0.035	0.034 ± 0.035
2160	0.040 ± 0.038	0.090 ± 0.035	-0.170 ± 0.041	-0.041 ± 0.039	0.045 ± 0.022	0.032 ± 0.036
2180	-0.116 ± 0.035	0.135 ± 0.035	-0.164 ± 0.035	-0.039 ± 0.035	0.045 ± 0.035	0.031 ± 0.035
W_0	D_{13}		D_{15}		F_{15}	
(MeV)	Re(D_{13})	Im(D_{13})	Re(D_{15})	Im(D_{15})	Re(F_{15})	Im(F_{15})
1480	0.000 ± 0.035	0.000 ± 0.035	-0.006 ± 0.035	-0.001 ± 0.035	0.000 ± 0.035	0.000 ± 0.035
1500	0.000 ± 0.035	0.000 ± 0.035	-0.010 ± 0.035	-0.002 ± 0.035	0.000 ± 0.035	0.000 ± 0.035
1520	0.000 ± 0.035	0.000 ± 0.035	-0.015 ± 0.035	-0.003 ± 0.035	0.000 ± 0.035	0.000 ± 0.035
1540	0.000 ± 0.035	0.000 ± 0.035	-0.021 ± 0.013	-0.004 ± 0.018	0.000 ± 0.035	0.000 ± 0.035
1560	-0.006 ± 0.018	0.005 ± 0.018	-0.029 ± 0.012	-0.005 ± 0.012	0.000 ± 0.035	0.000 ± 0.035
1580	-0.008 ± 0.016	0.010 ± 0.018	-0.038 ± 0.014	-0.008 ± 0.011	0.000 ± 0.035	0.000 ± 0.035
1600	-0.006 ± 0.015	0.014 ± 0.015	-0.048 ± 0.011	-0.011 ± 0.010	0.000 ± 0.035	0.000 ± 0.035
1620	-0.001 ± 0.026	0.022 ± 0.020	-0.071 ± 0.009	-0.016 ± 0.015	0.000 ± 0.035	0.000 ± 0.035
1640	0.002 ± 0.019	0.041 ± 0.015	-0.092 ± 0.005	-0.024 ± 0.012	0.000 ± 0.035	0.000 ± 0.035
1660	-0.018 ± 0.025	0.097 ± 0.016	-0.094 ± 0.011	-0.036 ± 0.014	0.000 ± 0.035	0.000 ± 0.035
1680	-0.052 ± 0.022	0.078 ± 0.014	-0.113 ± 0.012	-0.054 ± 0.015	0.000 ± 0.035	0.000 ± 0.035
1700	-0.048 ± 0.022	0.034 ± 0.024	-0.158 ± 0.016	-0.071 ± 0.026	0.000 ± 0.035	0.000 ± 0.035
1720	-0.088 ± 0.020	0.019 ± 0.017	-0.126 ± 0.020	-0.158 ± 0.019	-0.014 ± 0.016	-0.007 ± 0.012
1740	-0.088 ± 0.018	0.012 ± 0.016	-0.137 ± 0.022	-0.214 ± 0.016	-0.015 ± 0.014	-0.007 ± 0.011
1760	-0.086 ± 0.020	0.008 ± 0.018	-0.059 ± 0.028	-0.284 ± 0.015	-0.016 ± 0.016	-0.008 ± 0.013
1780	-0.088 ± 0.017	0.006 ± 0.016	0.029 ± 0.029	-0.291 ± 0.013	-0.018 ± 0.012	-0.009 ± 0.011
1800	-0.055 ± 0.019	0.004 ± 0.016	0.042 ± 0.030	-0.263 ± 0.013	-0.019 ± 0.014	-0.011 ± 0.012
1820	-0.094 ± 0.018	0.002 ± 0.016	0.110 ± 0.030	-0.226 ± 0.014	-0.021 ± 0.012	-0.015 ± 0.013

TABLE V. (*Continued*.)

W_0	D_{13}		D_{15}		F_{15}	
(MeV)	Re(D_{13})	Im(D_{13})	Re(D_{15})	Im(D_{15})	Re(F_{15})	Im(F_{15})
1840	-0.087 ± 0.018	-0.001 ± 0.016	0.109 ± 0.026	-0.175 ± 0.013	-0.021 ± 0.010	-0.021 ± 0.011
1860	-0.075 ± 0.025	-0.004 ± 0.022	0.109 ± 0.034	-0.127 ± 0.023	-0.019 ± 0.013	-0.028 ± 0.015
1880	-0.075 ± 0.019	-0.006 ± 0.017	0.119 ± 0.026	-0.116 ± 0.019	-0.012 ± 0.010	-0.035 ± 0.010
1900	-0.073 ± 0.023	-0.008 ± 0.023	0.123 ± 0.029	-0.105 ± 0.026	0.000 ± 0.015	-0.036 ± 0.016
1920	-0.066 ± 0.019	-0.009 ± 0.021	0.084 ± 0.017	-0.060 ± 0.020	0.011 ± 0.012	-0.028 ± 0.015
1940	-0.074 ± 0.015	-0.010 ± 0.019	0.089 ± 0.016	-0.074 ± 0.017	0.015 ± 0.010	-0.014 ± 0.013
1960	-0.060 ± 0.016	-0.011 ± 0.021	0.079 ± 0.018	-0.091 ± 0.018	0.017 ± 0.010	-0.004 ± 0.017
1980	-0.080 ± 0.031	-0.012 ± 0.026	0.072 ± 0.021	-0.049 ± 0.023	0.014 ± 0.021	0.006 ± 0.025
2000	-0.073 ± 0.029	-0.014 ± 0.027	0.094 ± 0.027	-0.028 ± 0.024	0.006 ± 0.023	0.015 ± 0.019
2020	-0.052 ± 0.035	-0.015 ± 0.035	0.121 ± 0.035	0.013 ± 0.035	-0.002 ± 0.035	0.020 ± 0.035
2040	-0.036 ± 0.035	-0.016 ± 0.035	0.087 ± 0.035	-0.005 ± 0.035	-0.011 ± 0.035	0.022 ± 0.035
2060	-0.065 ± 0.051	-0.018 ± 0.041	0.061 ± 0.044	-0.050 ± 0.038	-0.021 ± 0.044	0.021 ± 0.031
2080	-0.095 ± 0.045	-0.019 ± 0.043	0.083 ± 0.048	-0.049 ± 0.042	-0.030 ± 0.041	0.017 ± 0.032
2100	-0.120 ± 0.035	-0.020 ± 0.035	0.189 ± 0.035	-0.048 ± 0.035	-0.034 ± 0.035	0.014 ± 0.035
2120	-0.079 ± 0.048	-0.019 ± 0.051	0.054 ± 0.044	-0.046 ± 0.043	-0.035 ± 0.045	0.013 ± 0.037
2140	-0.081 ± 0.035	-0.018 ± 0.035	0.070 ± 0.035	-0.044 ± 0.035	-0.036 ± 0.035	0.012 ± 0.035
2160	-0.191 ± 0.022	-0.017 ± 0.038	-0.058 ± 0.023	-0.043 ± 0.030	-0.037 ± 0.022	0.009 ± 0.026
2180	-0.080 ± 0.035	-0.017 ± 0.035	0.071 ± 0.035	-0.041 ± 0.035	-0.039 ± 0.035	0.004 ± 0.035
W_0	F_{17}		G_{17}			
(MeV)	Re(F_{17})	Im(F_{17})	Re(G_{17})	Im(G_{17})		
1480	0.000 ± 0.035	0.000 ± 0.035	0.000	0.000		
1500	0.000 ± 0.035	0.000 ± 0.035	0.000	0.000		
1520	0.001 ± 0.035	0.000 ± 0.035	0.000	0.000		
1540	0.001 ± 0.011	0.000 ± 0.014	0.000	0.000		
1560	0.002 ± 0.005	0.000 ± 0.007	0.000	0.000		
1580	0.003 ± 0.005	0.000 ± 0.007	0.000	0.000		
1600	0.004 ± 0.006	0.000 ± 0.007	0.000	0.000		
1620	0.005 ± 0.008	0.000 ± 0.012	0.000	0.000		
1640	0.007 ± 0.006	0.000 ± 0.008	-0.001	0.000		
1660	0.009 ± 0.007	0.000 ± 0.008	-0.001	0.000		
1680	0.011 ± 0.006	0.000 ± 0.008	-0.001	0.000		
1700	0.014 ± 0.014	0.000 ± 0.026	-0.001	0.000		
1720	0.017 ± 0.015	0.001 ± 0.018	-0.001	-0.001		
1740	0.020 ± 0.017	0.001 ± 0.018	-0.001	-0.001		
1760	0.024 ± 0.022	0.001 ± 0.024	-0.001	-0.001		
1780	0.029 ± 0.022	0.002 ± 0.023	-0.002	-0.001		
1800	0.034 ± 0.023	0.003 ± 0.021	-0.002	-0.001		
1820	0.041 ± 0.023	0.004 ± 0.020	-0.003	-0.001		
1840	0.048 ± 0.022	0.005 ± 0.017	-0.003	-0.001		
1860	0.082 ± 0.026	0.008 ± 0.026	-0.004	-0.001		
1880	0.092 ± 0.019	0.013 ± 0.020	-0.004	-0.002		
1900	0.101 ± 0.022	0.021 ± 0.028	-0.005	-0.002		
1920	0.105 ± 0.014	0.035 ± 0.021	-0.006	-0.003		
1940	0.109 ± 0.014	0.052 ± 0.019	-0.007	-0.003		
1960	0.144 ± 0.014	0.045 ± 0.027	-0.008	-0.004		
1980	0.123 ± 0.025	0.104 ± 0.025	-0.009	-0.005		
2000	0.072 ± 0.033	0.140 ± 0.019	-0.010	-0.006		
2020	-0.021 ± 0.035	0.182 ± 0.035	-0.011	-0.007		
2040	0.018 ± 0.035	0.170 ± 0.035	-0.012	-0.008		
2060	-0.008 ± 0.044	0.147 ± 0.029	-0.013	-0.010		
2080	-0.026 ± 0.051	0.148 ± 0.032	-0.014	-0.012		
2100	-0.036 ± 0.035	0.159 ± 0.035	-0.015	-0.015		
2120	-0.040 ± 0.045	0.094 ± 0.033	-0.015	-0.017		
2140	-0.042 ± 0.035	0.102 ± 0.035	-0.014	-0.020		
2160	-0.042 ± 0.020	0.059 ± 0.021	-0.013	-0.022		
2180	-0.042 ± 0.035	0.084 ± 0.035	-0.012	-0.025		

TABLE VI. Summary of single-energy amplitudes for $\overline{K}N \to \pi\Sigma$.

W_0	S_{01}		P_{01}		P_{03}	
(MeV)	Re(S_{01})	Im(S_{01})	Re(P_{01})	Im(P_{01})	Re(P_{03})	Im(P_{03})
1480	-0.308 ± 0.035	0.316 ± 0.03	-0.036 ± 0.035	-0.019 ± 0.035	0.058 ± 0.035	-0.001 ± 0.035
1500	-0.285 ± 0.035	0.321 ± 0.035	-0.064 ± 0.035	-0.027 ± 0.035	0.062 ± 0.035	0.001 ± 0.035
1520	-0.268 ± 0.035	0.318 ± 0.035	-0.104 ± 0.035	-0.050 ± 0.035	0.063 ± 0.035	0.004 ± 0.035
1540	-0.206 ± 0.045	0.224 ± 0.040	-0.147 ± 0.039	-0.230 ± 0.044	0.147 ± 0.034	0.006 ± 0.041
1560	-0.280 ± 0.031	0.282 ± 0.032	-0.131 ± 0.031	-0.133 ± 0.037	0.119 ± 0.027	0.009 ± 0.030
1580	-0.242 ± 0.030	0.294 ± 0.028	-0.095 ± 0.028	-0.195 ± 0.033	0.121 ± 0.025	0.012 ± 0.027
1600	-0.253 ± 0.032	0.289 ± 0.029	-0.042 ± 0.029	-0.215 ± 0.034	0.105 ± 0.026	0.015 ± 0.027
1620	-0.251 ± 0.031	0.289 ± 0.032	-0.024 ± 0.029	-0.236 ± 0.034	0.108 ± 0.023	0.018 ± 0.029
1640	-0.296 ± 0.032	0.270 ± 0.034	-0.003 ± 0.029	-0.205 ± 0.037	0.128 ± 0.025	0.022 ± 0.030
1660	-0.307 ± 0.026	0.167 ± 0.031	-0.044 ± 0.027	-0.270 ± 0.029	0.140 ± 0.018	0.026 ± 0.027
1680	-0.132 ± 0.025	-0.091 ± 0.029	-0.032 ± 0.029	-0.222 ± 0.026	0.257 ± 0.020	0.031 ± 0.024
1700	-0.030 ± 0.036	-0.041 ± 0.036	-0.019 ± 0.038	-0.274 ± 0.029	0.188 ± 0.026	0.037 ± 0.031
1720	-0.032 ± 0.035	0.001 ± 0.038	-0.003 ± 0.039	-0.216 ± 0.029	0.101 ± 0.024	0.043 ± 0.034
1740	-0.027 ± 0.030	0.052 ± 0.032	0.019 ± 0.034	-0.187 ± 0.031	0.099 ± 0.021	0.068 ± 0.031
1760	-0.014 ± 0.033	0.018 ± 0.034	0.046 ± 0.036	-0.249 ± 0.029	0.139 ± 0.025	0.064 ± 0.031
1780	0.009 ± 0.032	0.031 ± 0.034	0.066 ± 0.036	-0.255 ± 0.027	0.137 ± 0.027	0.125 ± 0.026
1800	0.036 ± 0.035	0.019 ± 0.038	0.038 ± 0.041	-0.240 ± 0.034	0.148 ± 0.033	0.111 ± 0.030
1820	0.061 ± 0.052	0.017 ± 0.056	0.135 ± 0.056	-0.199 ± 0.057	0.118 ± 0.045	0.076 ± 0.046
1840	0.076 ± 0.030	0.013 ± 0.037	0.166 ± 0.037	-0.164 ± 0.036	0.114 ± 0.029	0.112 ± 0.028
1860	0.049 ± 0.025	0.002 ± 0.038	0.181 ± 0.038	-0.159 ± 0.036	0.137 ± 0.025	0.069 ± 0.029
1880	0.076 ± 0.029	-0.009 ± 0.040	0.160 ± 0.038	-0.121 ± 0.037	0.138 ± 0.020	0.060 ± 0.033
1900	0.147 ± 0.037	-0.018 ± 0.043	0.165 ± 0.041	0.005 ± 0.044	0.060 ± 0.030	0.017 ± 0.037
1920	0.094 ± 0.040	-0.025 ± 0.042	0.131 ± 0.046	-0.037 ± 0.044	0.107 ± 0.035	0.026 ± 0.031
1940	0.054 ± 0.052	-0.027 ± 0.059	0.132 ± 0.056	-0.118 ± 0.062	0.189 ± 0.041	0.015 ± 0.054
1960	0.045 ± 0.048	-0.027 ± 0.045	0.087 ± 0.047	0.036 ± 0.048	0.138 ± 0.039	0.035 ± 0.040
1980	0.052 ± 0.056	-0.025 ± 0.047	-0.008 ± 0.047	-0.026 ± 0.054	0.204 ± 0.051	0.056 ± 0.046
2000	0.099 ± 0.062	-0.022 ± 0.054	0.001 ± 0.051	-0.008 ± 0.059	0.176 ± 0.056	0.051 ± 0.052
2020	0.076 ± 0.033	-0.017 ± 0.029	0.029 ± 0.029	0.004 ± 0.032	0.160 ± 0.029	0.086 ± 0.029
2040	0.064 ± 0.035	-0.013 ± 0.035	0.006 ± 0.035	0.011 ± 0.035	0.131 ± 0.035	0.098 ± 0.035
2060	0.092 ± 0.045	-0.006 ± 0.047	-0.010 ± 0.043	0.016 ± 0.048	0.159 ± 0.040	0.158 ± 0.041
2080	0.116 ± 0.058	-0.002 ± 0.058	-0.028 ± 0.055	0.019 ± 0.059	0.120 ± 0.049	0.089 ± 0.048
2100	0.031 ± 0.035	0.002 ± 0.035	-0.044 ± 0.035	0.021 ± 0.035	0.204 ± 0.035	0.176 ± 0.035
2120	0.053 ± 0.043	0.007 ± 0.041	-0.024 ± 0.044	0.025 ± 0.044	0.072 ± 0.038	0.120 ± 0.034
2140	0.050 ± 0.035	0.012 ± 0.035	-0.065 ± 0.035	0.028 ± 0.035	0.104 ± 0.035	0.193 ± 0.035
2160	0.047 ± 0.047	0.014 ± 0.043	0.040 ± 0.043	0.027 ± 0.047	-0.018 ± 0.045	0.083 ± 0.041
2180	0.044 ± 0.035	0.016 ± 0.035	-0.092 ± 0.035	0.027 ± 0.035	0.076 ± 0.035	0.202 ± 0.035
W_0	D_{03}		D_{05}		F_{05}	
(MeV)	Re(D_{03})	Im(D_{03})	Re(D_{05})	Im(D_{05})	Re(F_{05})	Im(F_{05})
1480	0.038 ± 0.035	-0.005 ± 0.035	0.003 ± 0.035	0.002 ± 0.035	0.000 ± 0.035	0.000 ± 0.035
1500	0.113 ± 0.035	0.023 ± 0.035	0.002 ± 0.035	0.004 ± 0.035	0.000 ± 0.035	0.000 ± 0.035
1520	-0.025 ± 0.035	0.445 ± 0.035	0.000 ± 0.035	0.006 ± 0.035	-0.001 ± 0.035	0.000 ± 0.035
1540	-0.213 ± 0.029	0.098 ± 0.038	-0.003 ± 0.028	0.006 ± 0.028	-0.002 ± 0.031	0.000 ± 0.035
1560	-0.109 ± 0.027	0.028 ± 0.034	-0.006 ± 0.025	0.005 ± 0.026	-0.003 ± 0.023	0.000 ± 0.029
1580	-0.117 ± 0.024	0.011 ± 0.031	-0.009 ± 0.022	0.004 ± 0.023	-0.004 ± 0.021	0.000 ± 0.024
1600	-0.138 ± 0.025	0.000 ± 0.031	-0.013 ± 0.022	0.003 ± 0.022	-0.006 ± 0.024	0.000 ± 0.024
1620	-0.149 ± 0.024	-0.015 ± 0.029	-0.016 ± 0.020	0.002 ± 0.021	-0.009 ± 0.023	0.000 ± 0.023
1640	-0.169 ± 0.026	-0.041 ± 0.029	-0.021 ± 0.020	0.001 ± 0.021	-0.014 ± 0.022	-0.001 ± 0.023
1660	-0.241 ± 0.019	-0.040 ± 0.026	-0.026 ± 0.015	0.000 ± 0.021	-0.019 ± 0.020	-0.002 ± 0.018
1680	-0.104 ± 0.020	-0.239 ± 0.018	-0.032 ± 0.017	-0.003 ± 0.018	-0.028 ± 0.015	-0.003 ± 0.017
1700	0.018 ± 0.029	-0.248 ± 0.024	-0.040 ± 0.025	-0.006 ± 0.024	-0.039 ± 0.027	-0.007 ± 0.023
1720	0.079 ± 0.027	-0.077 ± 0.028	-0.050 ± 0.021	-0.012 ± 0.031	-0.095 ± 0.025	-0.013 ± 0.027
1740	0.109 ± 0.024	-0.100 ± 0.025	-0.057 ± 0.015	-0.023 ± 0.025	-0.133 ± 0.021	-0.027 ± 0.026
1760	0.060 ± 0.027	-0.048 ± 0.025	-0.059 ± 0.018	-0.041 ± 0.023	-0.119 ± 0.025	-0.057 ± 0.024
1780	0.029 ± 0.031	-0.032 ± 0.022	-0.066 ± 0.021	-0.062 ± 0.021	-0.128 ± 0.026	-0.103 ± 0.019
1800	0.087 ± 0.035	-0.020 ± 0.025	-0.070 ± 0.028	-0.091 ± 0.024	-0.111 ± 0.029	-0.163 ± 0.024
1820	0.157 ± 0.049	-0.008 ± 0.042	-0.026 ± 0.041	-0.166 ± 0.036	0.005 ± 0.045	-0.236 ± 0.036

TABLE VI. (*Continued*.)

W_0	D_{03}		D_{05}		F_{05}	
(MeV)	Re(D_{03})	Im(D_{03})	Re(D_{05})	Im(D_{05})	Re(F_{05})	Im(F_{05})
1840	0.113 ± 0.031	0.004 ± 0.027	0.035 ± 0.021	-0.112 ± 0.023	0.084 ± 0.026	-0.213 ± 0.021
1860	0.075 ± 0.032	0.018 ± 0.027	0.050 ± 0.023	-0.082 ± 0.025	0.106 ± 0.028	-0.194 ± 0.023
1880	0.050 ± 0.027	0.033 ± 0.028	0.090 ± 0.017	-0.044 ± 0.026	0.207 ± 0.020	-0.079 ± 0.023
1900	0.102 ± 0.035	0.048 ± 0.038	0.096 ± 0.028	-0.030 ± 0.032	0.146 ± 0.031	-0.082 ± 0.029
1920	0.070 ± 0.039	0.090 ± 0.037	0.086 ± 0.031	-0.048 ± 0.025	0.169 ± 0.032	-0.078 ± 0.028
1940	0.061 ± 0.043	-0.015 ± 0.059	0.115 ± 0.047	-0.038 ± 0.038	0.116 ± 0.030	-0.045 ± 0.047
1960	0.081 ± 0.041	0.077 ± 0.045	0.087 ± 0.040	-0.030 ± 0.030	0.162 ± 0.034	-0.029 ± 0.037
1980	0.113 ± 0.045	0.085 ± 0.053	0.065 ± 0.048	-0.025 ± 0.045	0.126 ± 0.043	-0.016 ± 0.044
2000	0.113 ± 0.049	0.084 ± 0.058	0.090 ± 0.052	-0.020 ± 0.052	0.143 ± 0.045	-0.005 ± 0.047
2020	0.103 ± 0.031	0.065 ± 0.032	0.081 ± 0.028	-0.016 ± 0.026	0.155 ± 0.027	0.004 ± 0.027
2040	0.105 ± 0.035	0.041 ± 0.035	0.043 ± 0.035	-0.013 ± 0.035	0.126 ± 0.035	0.011 ± 0.035
2060	0.105 ± 0.043	0.054 ± 0.046	0.043 ± 0.037	-0.011 ± 0.039	0.178 ± 0.036	0.017 ± 0.040
2080	0.085 ± 0.052	0.084 ± 0.054	0.049 ± 0.048	-0.009 ± 0.046	0.126 ± 0.048	0.021 ± 0.046
2100	-0.040 ± 0.035	0.134 ± 0.035	0.046 ± 0.035	-0.007 ± 0.035	0.171 ± 0.035	0.023 ± 0.035
2120	0.072 ± 0.042	0.046 ± 0.038	0.044 ± 0.037	-0.005 ± 0.033	0.102 ± 0.036	0.026 ± 0.030
2140	0.043 ± 0.035	0.132 ± 0.035	0.042 ± 0.035	-0.004 ± 0.035	0.080 ± 0.035	0.027 ± 0.035
2160	0.036 ± 0.042	0.056 ± 0.041	0.040 ± 0.040	-0.003 ± 0.037	0.120 ± 0.036	0.027 ± 0.037
2180	0.028 ± 0.035	0.134 ± 0.035	0.038 ± 0.035	-0.002 ± 0.035	0.069 ± 0.035	0.027 ± 0.035
W_0	F_{07}		G_{07}			
(MeV)	Re(F_{07})		Re(F_{07})	Im(G_{07})		
1480	0.000 ± 0.035	0.000 ± 0.035	0.000 ± 0.035	0.000 ± 0.035		
1500	0.000 ± 0.035	0.000 ± 0.035	0.000 ± 0.035	0.000 ± 0.035		
1520	0.000 ± 0.035	0.000 ± 0.035	0.000 ± 0.035	0.000 ± 0.035		
1540	0.000 ± 0.022	0.000 ± 0.027	0.000 ± 0.035	0.000 ± 0.035		
1560	0.000 ± 0.011	0.000 ± 0.015	0.000 ± 0.035	0.000 ± 0.035		
1580	0.000 ± 0.011	0.000 ± 0.014	0.000 ± 0.035	0.000 ± 0.035		
1600	0.001 ± 0.013	0.000 ± 0.014	0.000 ± 0.035	0.000 ± 0.035		
1620	0.001 ± 0.012	0.000 ± 0.016	0.000 ± 0.035	0.000 ± 0.035		
1640	0.002 ± 0.012	0.000 ± 0.016	0.000 ± 0.035	0.000 ± 0.035		
1660	0.002 ± 0.012	0.000 ± 0.016	0.000 ± 0.035	0.000 ± 0.035		
1680	0.003 ± 0.010	0.000 ± 0.014	0.000 ± 0.035	0.000 ± 0.035		
1700	0.004 ± 0.019	0.000 ± 0.021	0.000 ± 0.035	0.000 ± 0.035		
1720	0.006 ± 0.018	0.000 ± 0.025	0.000 ± 0.035	0.000 ± 0.035		
1740	0.008 ± 0.017	0.000 ± 0.022	0.000 ± 0.035	0.000 ± 0.035		
1760	0.010 ± 0.021	0.000 ± 0.019	0.000 ± 0.035	0.000 ± 0.035		
1780	0.012 ± 0.024	0.000 ± 0.015	0.000 ± 0.035	0.000 ± 0.035		
1800	0.015 ± 0.030	0.000 ± 0.017	0.000 ± 0.035	0.000 ± 0.035		
1820	0.018 ± 0.040	0.001 ± 0.033	0.000 ± 0.035	0.000 ± 0.035		
1840	0.022 ± 0.023	0.001 ± 0.023	0.000 ± 0.035	0.000 ± 0.035		
1860	0.027 ± 0.019	0.002 ± 0.025	0.000 ± 0.035	0.000 ± 0.035		
1880	0.032 ± 0.018	0.003 ± 0.025	0.000 ± 0.035	0.000 ± 0.035		
1900	0.038 ± 0.022	0.004 ± 0.030	0.000 ± 0.035	0.000 ± 0.035		
1920	0.045 ± 0.027	0.006 ± 0.028	0.000 ± 0.035	0.000 ± 0.035		
1940	0.055 ± 0.024	0.010 ± 0.037	0.000 ± 0.035	0.000 ± 0.035		
1960	0.054 ± 0.029	0.014 ± 0.032	0.000 ± 0.035	0.000 ± 0.035		
1980	0.088 ± 0.039	0.021 ± 0.038	0.000 ± 0.035	0.000 ± 0.035		
2000	0.137 ± 0.042	0.031 ± 0.043	0.000 ± 0.035	0.000 ± 0.035		
2020	0.088 ± 0.027	0.045 ± 0.019	0.000 ± 0.035	0.000 ± 0.035		
2040	0.111 ± 0.035	0.053 ± 0.035	0.000 ± 0.035	0.000 ± 0.035		
2060	0.069 ± 0.038	0.073 ± 0.031	0.000 ± 0.035	0.000 ± 0.035		
2080	0.115 ± 0.049	0.130 ± 0.041	0.000 ± 0.035	0.000 ± 0.035		
2100	0.145 ± 0.035	0.118 ± 0.035	0.000 ± 0.035	0.000 ± 0.035		
2120	0.100 ± 0.038	0.126 ± 0.025	0.000 ± 0.035	0.000 ± 0.035		
2140	0.042 ± 0.035	0.101 ± 0.035	0.000 ± 0.035	0.000 ± 0.035		
2160	0.036 ± 0.035	0.152 ± 0.032	0.000 ± 0.035	0.000 ± 0.035		
2180	0.033 ± 0.035	0.094 ± 0.035	0.000 ± 0.035	0.000 ± 0.035		

TABLE VI. (*Continued*.)

W_0	S_{11}		P_{11}		P_{13}	
(MeV)	Re(S_{11})	Im(S_{11})	Re(P_{11})	Im(P_{11})	Re(P_{13})	Im(P_{13})
1480	0.188 ± 0.035	0.282 ± 0.035	0.001 ± 0.035	-0.012 ± 0.035	0.060 ± 0.035	-0.011 ± 0.035
1500	0.174 ± 0.035	0.290 ± 0.035	-0.010 ± 0.035	-0.015 ± 0.035	0.068 ± 0.035	-0.014 ± 0.035
1520	0.170 ± 0.035	0.288 ± 0.035	-0.027 ± 0.035	-0.022 ± 0.035	0.070 ± 0.035	-0.017 ± 0.035
1540	0.151 ± 0.039	0.316 ± 0.026	-0.041 ± 0.039	-0.032 ± 0.041	0.035 ± 0.033	-0.019 ± 0.034
1560	0.168 ± 0.027	0.283 ± 0.025	-0.049 ± 0.029	-0.041 ± 0.037	0.066 ± 0.023	-0.021 ± 0.027
1580	0.190 ± 0.028	0.332 ± 0.022	0.006 ± 0.027	-0.077 ± 0.033	0.034 ± 0.023	-0.023 ± 0.026
1600	0.154 ± 0.031	0.325 ± 0.020	-0.013 ± 0.026	-0.034 ± 0.033	0.039 ± 0.024	-0.028 ± 0.024
1620	0.182 ± 0.027	0.266 ± 0.026	-0.041 ± 0.026	-0.072 ± 0.031	0.074 ± 0.021	-0.031 ± 0.027
1640	0.175 ± 0.032	0.287 ± 0.026	-0.001 ± 0.025	-0.069 ± 0.033	0.065 ± 0.023	-0.033 ± 0.029
1660	0.186 ± 0.025	0.201 ± 0.033	-0.040 ± 0.024	-0.137 ± 0.024	0.070 ± 0.019	-0.029 ± 0.027
1680	0.079 ± 0.025	0.226 ± 0.025	-0.015 ± 0.028	-0.057 ± 0.016	0.110 ± 0.018	-0.025 ± 0.017
1700	0.090 ± 0.033	0.182 ± 0.033	0.029 ± 0.036	-0.105 ± 0.026	0.109 ± 0.022	-0.022 ± 0.026
1720	0.171 ± 0.033	0.168 ± 0.037	0.044 ± 0.039	-0.163 ± 0.028	0.146 ± 0.022	-0.019 ± 0.034
1740	0.214 ± 0.028	0.171 ± 0.029	0.000 ± 0.034	-0.125 ± 0.026	0.109 ± 0.018	-0.016 ± 0.028
1760	0.206 ± 0.031	0.044 ± 0.031	0.052 ± 0.035	-0.112 ± 0.027	0.083 ± 0.022	-0.014 ± 0.027
1780	0.186 ± 0.029	0.048 ± 0.030	0.090 ± 0.034	-0.040 ± 0.024	0.090 ± 0.023	-0.011 ± 0.023
1800	0.238 ± 0.032	0.035 ± 0.032	0.102 ± 0.039	-0.029 ± 0.031	0.092 ± 0.028	-0.011 ± 0.025
1820	0.174 ± 0.046	0.094 ± 0.046	0.191 ± 0.051	-0.019 ± 0.053	0.105 ± 0.039	-0.013 ± 0.039
1840	0.220 ± 0.026	0.107 ± 0.033	0.044 ± 0.036	-0.010 ± 0.035	0.094 ± 0.023	-0.018 ± 0.023
1860	0.256 ± 0.023	0.076 ± 0.034	0.039 ± 0.038	-0.004 ± 0.035	0.096 ± 0.024	-0.025 ± 0.026
1880	0.156 ± 0.027	0.134 ± 0.037	0.036 ± 0.033	-0.003 ± 0.034	0.148 ± 0.019	-0.031 ± 0.025
1900	0.167 ± 0.037	0.160 ± 0.040	0.035 ± 0.037	-0.003 ± 0.041	0.143 ± 0.025	-0.036 ± 0.030
1920	0.106 ± 0.037	0.137 ± 0.037	0.035 ± 0.042	-0.004 ± 0.043	0.081 ± 0.030	-0.038 ± 0.021
1940	0.009 ± 0.044	0.094 ± 0.058	0.034 ± 0.045	-0.004 ± 0.057	0.147 ± 0.037	-0.039 ± 0.047
1960	-0.028 ± 0.043	0.047 ± 0.040	0.035 ± 0.041	-0.003 ± 0.048	0.147 ± 0.034	-0.039 ± 0.036
1980	-0.045 ± 0.053	0.032 ± 0.043	0.037 ± 0.041	-0.002 ± 0.051	0.130 ± 0.047	-0.039 ± 0.039
2000	-0.044 ± 0.059	-0.010 ± 0.050	0.038 ± 0.044	-0.001 ± 0.056	0.145 ± 0.050	-0.037 ± 0.045
2020	-0.035 ± 0.031	-0.041 ± 0.026	0.038 ± 0.026	0.001 ± 0.029	0.081 ± 0.026	-0.036 ± 0.026
2040	-0.023 ± 0.035	-0.102 ± 0.035	0.037 ± 0.035	0.003 ± 0.035	0.113 ± 0.035	-0.035 ± 0.035
2060	-0.011 ± 0.043	-0.058 ± 0.046	0.033 ± 0.039	0.005 ± 0.047	0.052 ± 0.035	-0.032 ± 0.035
2080	-0.001 ± 0.056	-0.110 ± 0.054	0.030 ± 0.050	0.008 ± 0.055	0.055 ± 0.049	-0.031 ± 0.043
2100	0.008 ± 0.035	-0.051 ± 0.035	0.026 ± 0.035	0.009 ± 0.035	0.100 ± 0.035	-0.030 ± 0.035
2120	0.015 ± 0.042	-0.108 ± 0.035	0.019 ± 0.041	0.010 ± 0.042	0.067 ± 0.035	-0.028 ± 0.029
2140	0.023 ± 0.035	-0.096 ± 0.035	0.011 ± 0.035	0.011 ± 0.035	0.096 ± 0.035	-0.026 ± 0.035
2160	0.029 ± 0.046	-0.127 ± 0.041	0.006 ± 0.041	0.012 ± 0.044	0.019 ± 0.042	-0.025 ± 0.037
2180	0.034 ± 0.035	-0.100 ± 0.035	0.001 ± 0.035	0.012 ± 0.035	0.094 ± 0.035	-0.024 ± 0.035
W_0	D_{13}		D_{15}		F_{15}	
(MeV)	Re(D_{13})	Im(D_{13})	Re(D_{15})	Im(D_{15})	Re(F_{15})	Im(F_{15})
1480	0.000 ± 0.035	0.000 ± 0.035	0.003 ± 0.035	-0.002 ± 0.035	0.000 ± 0.035	0.000 ± 0.035
1500	0.000 ± 0.035	0.000 ± 0.035	0.005 ± 0.035	-0.003 ± 0.035	0.000 ± 0.035	0.000 ± 0.035
1520	0.000 ± 0.035	0.000 ± 0.035	0.007 ± 0.035	-0.004 ± 0.035	0.000 ± 0.035	0.000 ± 0.035
1540	0.000 ± 0.035	0.000 ± 0.035	0.009 ± 0.028	-0.006 ± 0.023	0.000 ± 0.035	0.000 ± 0.035
1560	0.006 ± 0.025	0.001 ± 0.033	0.012 ± 0.021	-0.007 ± 0.024	0.000 ± 0.035	0.000 ± 0.035
1580	0.023 ± 0.024	0.002 ± 0.031	0.016 ± 0.021	-0.009 ± 0.023	0.000 ± 0.035	0.000 ± 0.035
1600	0.040 ± 0.024	0.009 ± 0.030	0.020 ± 0.020	-0.010 ± 0.022	0.000 ± 0.035	0.000 ± 0.035
1620	0.073 ± 0.023	0.027 ± 0.027	0.026 ± 0.018	-0.012 ± 0.022	0.000 ± 0.035	0.000 ± 0.035
1640	0.106 ± 0.026	0.054 ± 0.028	0.034 ± 0.019	-0.012 ± 0.024	0.000 ± 0.035	0.000 ± 0.035
1660	0.105 ± 0.018	0.156 ± 0.025	0.041 ± 0.018	-0.011 ± 0.020	0.000 ± 0.035	0.000 ± 0.035
1680	-0.051 ± 0.019	0.177 ± 0.015	0.048 ± 0.017	-0.006 ± 0.013	0.000 ± 0.035	0.000 ± 0.035
1700	-0.135 ± 0.025	0.106 ± 0.024	0.063 ± 0.022	0.004 ± 0.018	0.000 ± 0.035	0.000 ± 0.035
1720	-0.141 ± 0.025	0.043 ± 0.029	0.077 ± 0.015	0.020 ± 0.025	-0.018 ± 0.022	-0.001 ± 0.027
1740	-0.066 ± 0.021	0.021 ± 0.025	0.082 ± 0.011	0.047 ± 0.020	-0.023 ± 0.019	-0.004 ± 0.023
1760	-0.080 ± 0.024	0.009 ± 0.023	0.074 ± 0.015	0.101 ± 0.019	-0.030 ± 0.023	-0.007 ± 0.022
1780	-0.091 ± 0.027	0.002 ± 0.020	0.029 ± 0.018	0.128 ± 0.015	-0.039 ± 0.025	-0.013 ± 0.017
1800	-0.058 ± 0.032	-0.001 ± 0.024	0.004 ± 0.024	0.126 ± 0.019	-0.049 ± 0.025	-0.023 ± 0.023
1820	-0.047 ± 0.048	-0.002 ± 0.038	-0.011 ± 0.035	0.101 ± 0.030	-0.009 ± 0.041	-0.039 ± 0.036

TABLE VI. (*Continued*.)

W_0	D_{13}		D_{15}		F_{15}	
(MeV)	Re(D_{13})	Im(D_{13})	Re(D_{15})	Im(D_{15})	Re(F_{15})	Im(F_{15})
1840	-0.038 ± 0.029	-0.002 ± 0.024	-0.018 ± 0.020	0.083 ± 0.019	-0.042 ± 0.023	-0.021 ± 0.020
1860	-0.030 ± 0.031	0.000 ± 0.024	-0.021 ± 0.021	0.049 ± 0.020	-0.043 ± 0.025	-0.008 ± 0.021
1880	-0.022 ± 0.026	0.002 ± 0.026	-0.021 ± 0.019	0.041 ± 0.021	-0.033 ± 0.020	-0.075 ± 0.019
1900	-0.017 ± 0.032	0.003 ± 0.036	-0.019 ± 0.028	0.034 ± 0.026	-0.014 ± 0.029	-0.142 ± 0.026
1920	-0.014 ± 0.037	0.004 ± 0.034	-0.016 ± 0.032	0.027 ± 0.021	0.033 ± 0.030	-0.155 ± 0.023
1940	-0.012 ± 0.034	0.005 ± 0.051	-0.012 ± 0.051	0.020 ± 0.032	0.064 ± 0.025	-0.091 ± 0.037
1960	-0.009 ± 0.038	0.005 ± 0.042	-0.008 ± 0.040	0.017 ± 0.022	0.084 ± 0.034	-0.136 ± 0.030
1980	-0.005 ± 0.042	0.006 ± 0.049	-0.004 ± 0.041	0.013 ± 0.040	0.081 ± 0.039	-0.098 ± 0.038
2000	-0.002 ± 0.044	0.006 ± 0.052	0.000 ± 0.042	0.007 ± 0.045	0.089 ± 0.041	-0.085 ± 0.041
2020	0.001 ± 0.028	0.007 ± 0.031	0.005 ± 0.026	0.003 ± 0.024	0.122 ± 0.024	-0.089 ± 0.025
2040	0.003 ± 0.035	0.007 ± 0.035	0.011 ± 0.035	0.000 ± 0.035	0.126 ± 0.035	-0.038 ± 0.035
2060	0.003 ± 0.040	0.007 ± 0.044	0.018 ± 0.031	-0.004 ± 0.034	0.162 ± 0.032	-0.022 ± 0.036
2080	0.003 ± 0.049	0.008 ± 0.051	0.026 ± 0.040	-0.006 ± 0.038	0.105 ± 0.044	-0.013 ± 0.040
2100	0.004 ± 0.035	0.008 ± 0.035	0.033 ± 0.035	-0.006 ± 0.035	0.089 ± 0.035	-0.005 ± 0.035
2120	0.007 ± 0.039	0.007 ± 0.036	0.040 ± 0.030	-0.004 ± 0.025	0.120 ± 0.034	0.007 ± 0.029
2140	0.009 ± 0.035	0.006 ± 0.035	0.049 ± 0.035	-0.001 ± 0.035	0.104 ± 0.035	0.017 ± 0.035
2160	0.010 ± 0.037	0.006 ± 0.037	0.107 ± 0.035	0.005 ± 0.031	0.085 ± 0.034	0.023 ± 0.033
2180	0.011 ± 0.035	0.006 ± 0.035	0.064 ± 0.035	0.011 ± 0.035	0.091 ± 0.035	0.025 ± 0.035
W_0	F_{17}		G_{17}			
(MeV)	Re(F_{17})	Im(F_{17})	Re(G_{17})	Im(G_{17})		
1480	0.000 ± 0.035	0.000 ± 0.035	0.000	0.000		
1500	0.000 ± 0.035	0.000 ± 0.035	0.000	0.000		
1520	0.000 ± 0.035	0.000 ± 0.035	0.000	0.000		
1540	0.000 ± 0.017	0.000 ± 0.020	0.000	0.000		
1560	0.000 ± 0.014	0.000 ± 0.014	-0.001	0.000		
1580	0.000 ± 0.015	0.000 ± 0.014	-0.001	0.000		
1600	0.000 ± 0.015	0.000 ± 0.012	-0.002	-0.001		
1620	0.000 ± 0.013	0.000 ± 0.014	-0.003	-0.001		
1640	0.000 ± 0.015	0.000 ± 0.015	-0.004	-0.003		
1660	0.000 ± 0.014	0.000 ± 0.016	-0.003	-0.004		
1680	-0.001 ± 0.015	0.000 ± 0.010	-0.003	-0.005		
1700	-0.001 ± 0.020	0.000 ± 0.016	-0.002	-0.006		
1720	-0.002 ± 0.014	0.000 ± 0.018	0.000	-0.007		
1740	-0.004 ± 0.011	0.001 ± 0.017	0.001	-0.007		
1760	-0.005 ± 0.014	0.001 ± 0.019	0.002	-0.008		
1780	-0.008 ± 0.018	0.001 ± 0.014	0.004	-0.008		
1800	-0.011 ± 0.020	0.002 ± 0.018	0.006	-0.008		
1820	-0.016 ± 0.032	0.002 ± 0.023	0.008	-0.009		
1840	-0.021 ± 0.017	0.001 ± 0.014	0.010	-0.009		
1860	-0.028 ± 0.019	-0.001 ± 0.015	0.013	-0.009		
1880	-0.036 ± 0.010	-0.005 ± 0.018	0.016	-0.010		
1900	-0.046 ± 0.019	-0.011 ± 0.020	0.019	-0.010		
1920	-0.036 ± 0.023	-0.023 ± 0.020	0.023	-0.009		
1940	-0.078 ± 0.032	-0.039 ± 0.032	0.027	-0.009		
1960	-0.041 ± 0.027	-0.026 ± 0.019	0.032	-0.008		
1980	-0.023 ± 0.029	-0.046 ± 0.026	0.037	-0.007		
2000	-0.035 ± 0.025	-0.042 ± 0.034	0.043	-0.006		
2020	-0.012 ± 0.023	-0.082 ± 0.020	0.050	-0.004		
2040	0.010 ± 0.035	-0.103 ± 0.035	0.098	-0.001		
2060	0.026 ± 0.029	-0.077 ± 0.030	0.070	0.004		
2080	0.035 ± 0.037	-0.073 ± 0.038	0.079	0.009		
2100	0.040 ± 0.035	-0.026 ± 0.035	0.057	0.017		
2120	0.041 ± 0.031	-0.057 ± 0.026	0.080	0.026		
2140	0.041 ± 0.035	-0.056 ± 0.035	0.088	0.037		
2160	0.039 ± 0.033	-0.050 ± 0.026	0.078	0.050		
2180	0.038 ± 0.035	-0.045 ± 0.035	0.090	0.062		

[1] R. Armenteros *et al*., Nucl. Phys. B **14**, 91 (1969).
[2] B. Conforto, D. M. Harmsen, T. Lasinski, R. Levi-Setti, M. Raymund, E. Burkhardt, H. Filthuth, S. Klein, H. Oberlack, and H. Schleich, Nucl. Phys. B **34**, 41 (1971).
[3] A. J. Van Horn, Nucl. Phys. B **87**, 145 (1975).
[4] R. J. Hemingway, J. Eades, D. M. Harmsen, J. O. Petersen, A. Putzer, C. M. Kiesling, D. E. Plane, and W. Wittek, Nucl. Phys. B **91**, 12 (1975).
[5] P. Baillon and P. J. Litchfield, Nucl. Phys. B **94**, 39 (1975).
[6] G. P. Gopal, R. T. Ross, A. J. Van Horn, A. C. McPherson, E. F. Clayton, T. C. Bacon, and I. Butterworth, Nucl. Phys. B **119**, 362 (1977).
[7] H. Zhang, J. Tulpan, M. Shrestha, and D. M. Manley, following paper, Phys. Rev. C **88**, 035205 (2013).
[8] See, for example, B. H. Bransden and R. Gordon Moorhouse, *The Pion-Nucleon System* (Princeton University Press, Princeton, 1973).
[9] T. S. Mast, M. Alston-Garnjost, R. O. Bangerter, A. S. Barbaro-Galtieri, F. T. Solmitz, and R. D. Tripp, Phys. Rev. D **14**, 13 (1976).
[10] R. Armenteros, P. Baillon, C. Bricman, M. Ferro-Luzzi, E. Pagiola, J. O. Petersen, D. E. Plane, N. Schmitz, E. Burkhardt, and H. Filthuth, Nucl. Phys. B **21**, 15 (1970).
[11] M. Alston-Garnjost, R.W. Kenney, D. L. Pollard, R. R. Ross, R. D. Tripp, and H. Nicholson, Phys. Rev. D **17**, 2226 (1978).
[12] S. Prakhov *et al*., Phys. Rev. C **80**, 025204 (2009).
[13] C. J. Adams *et al*., Nucl. Phys. B **96**, 54 (1975).
[14] R. Armenteros *et al*., Nucl. Phys. B **8**, 233 (1968).
[15] M. G. Albrow, S. Andersson-Almehed, B. Bošnjakovic, F. C. Erné, Y. Kimura, J. P. Lagnaux, J. C. Sens, and F. Udo, Nucl. Phys. B **29**, 413 (1971).
[16] M. Jones, R. Levi-Setti, D. Merrill, and R. D. Tripp, Nucl. Phys. B **90**, 349 (1975).
[17] S. Andersson-Almehed, C. Daum, F. C. Erné, J. P. Lagnaux, J. C. Sens, and F. Udo, Nucl. Phys. B **21**, 515 (1970).
[18] B. Conforto, G. P. Gopal, G. E. Kalmus, P. J. Litchfield, R. T. Ross, A. J. Van Horn, T. C. Bacon, I. Butterworth, E. F. Clayton, and R. M. Waters, Nucl. Phys. B **105**, 189 (1976).
[19] J. Griselin *et al*., Nucl. Phys. B **93**, 189 (1975).
[20] C. Daum, F. C. Erné, J. P. Lagnaux, J. C. Sens, M. Steuer, and F. Udo, Nucl. Phys. B **6**, 273 (1968).
[21] K. Abe, B. A. Barnett, J. H. Goldman, A. T. Laasanen, P. H. Steinberg, G. J. Marmer, D. R. Moffett, and E. F. Parker, Phys. Rev. D **12**, 6 (1975).
[22] A. Baldini, V. Flaminio, W. G. Moorhead, and D. R. O. Morrison, *Total Cross-Sections for Reactions of High Energy Particles*, Landolt-Börnstein Numerical Data and Functional Relationships in Science and Technology, Vol. 12 (Springer-Verlag, Berlin, 1988).
[23] D. F. Baxter *et al*., Nucl. Phys. B **67**, 125 (1973).
[24] A. Berthon, L. K. Rangan, J. Vrana, I. Butterworth, P. J. Litchfield, A. M. Segar, J. R. Smith, J. Meyer, E. Pauli, and B. Tallini, Nucl. Phys. B **20**, 476 (1970); A. Berton, J. Vrana, I. Butterworth, P. J. Litchfield, J. R. Smith, J. Meyer, E. Pauli, and B. Tallini, *ibid*. **24**, 417 (1970).
[25] G. W. London *et al*., Nucl. Phys. B **85**, 289 (1975).
[26] R. W. Manweiler *et al*., Phys. Rev. C **77**, 015205 (2008).
[27] J. Tulpan, Ph.D. dissertation, Kent State University 2007 (unpublished).
[28] A. Starostin *et al*., Phys. Rev. C **64**, 055205 (2001).
[29] M. Shrestha and D. M. Manley, Phys. Rev. C **86**, 055203 (2012).
[30] W. Cameron *et al*., Nucl. Phys. B **143**, 189 (1978).
[31] W. Cameron *et al*., Nucl. Phys. B **131**, 399 (1977).
[32] W. Cameron *et al*., Nucl. Phys. B **146**, 327 (1978).
[33] P. J. Litchfield, R. J. Hemingway, P. Baillon, A. Albrecht, and A. Putzer, Nucl. Phys. B **74**, 39 (1974).
[34] See Supplemental Material at http://link.aps.org/supplemental/10.1103/PhysRevC.88.035204 for data files containing all the single-energy partial-wave amplitudes listed in this paper.